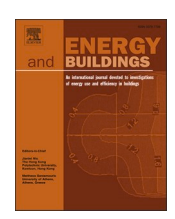
ELSEVIER

Contents lists available at ScienceDirect

Energy & Buildings

journal homepage: www.elsevier.com/locate/enb





Comprehensive analysis of energy and visual performance of building-integrated photovoltaics in all ASHRAE climate zones

Hamideh Hossei a,*, Kyoung Hee Kim b

- ^a Department of Infrastructure and Environmental System, UNC Charlotte, 9201 University City Blvd, Charlotte, NC, 28223, USA
- ^b School of Architecture, UNC Charlotte, 9201 University City Blvd, Charlotte, NC, 28223, USA

ARTICLE INFO

Keywords: South façade PV-louvers and PV-mounted roof potential power production BIPV energy consumption ASHRAE climate zones BIPVs net energy

ABSTRACT

Integrating PV panels into building facades (BIPV) necessitates a comprehensive understanding of the PV system's impact on building energy consumption within the site's climate zone. Maximizing PV power output depends on factors such as location, climate type, and latitude. However, minimizing total electricity consumption, which includes cooling, heating, and lighting loads, is significantly influenced by the design of the PV system and the climate region. This study conducted a thorough evaluation of the impact of south-facing PVintegrated louvers on both PV power generation and building energy performance, as well as occupants' visual comfort, across 17 ASHRAE climate regions in the U.S. The results indicated that south-facing PV-integrated louvers significantly reduced building energy consumption in climate zones 1 to 3, as well as 4B and 5B. Wider louvers with longer spacing (S-3 typology) were particularly effective in zones with moderate cooling needs (climate zone 4). However, in colder climates (6-8) with significant heating demands, roof-mounted systems provided a better balance between power generation and solar heat gain for the building. The PV-louver designs effectively reduced sunlight penetration and maintained illuminance levels within the desired range across most of the floor area. Conversely, roof typologies exhibited lower lighting loads but resulted in significantly high mean illuminance levels on the working surface, leading to disturbing glare for occupants across a large portion of the floor area. The findings of this research offer practical implications for architects, engineers, and policymakers seeking sustainable building solutions.

1. Introduction

Residential and commercial buildings consumed 22 % and 18 % of the total energy in the U.S. in 2022 [1]. Integrating PV panels into building roofs is the most common method to offset grid electricity consumption in residential and small to medium commercial buildings. While roof installation is more benefitial for buildings up to 6 story height [2], in case of buildings with a significant facade-to-roof ratio, facades offer larger active surfaces for PV panel integration [3]. In addition to maximizing PV system power production, reducing building energy consumption plays a vital role in addressing the building sector's reliance on fossil fuel-based electricity. To achieve net-zero (NZE) and net-positive BIPVs, the PV system should not only generate on-site electricity but also decrease the building's overall energy consumption while ensuring visual comfort for occupants.

While the building facade offers an excellent opportunity for harnessing solar energy and installing PV panels, understanding the impact

of BIPV facade systems on overall building performance is crucial. The overall energy consumption of a building is influenced by three performance metrics: cooling, heating, and lighting loads (Fig. 1). Vertical PV system design parameters, including the distance, number, length, and width of the PV panels, PV modules tilt angle as well as site condition such as the building's geographical location, latitude, weather condition and facade orientation, affects these performance metrics differently. Consequently, achieving a balance among all performance metrics and the PVPP will result in the optimal BIPV component combination.

1.1. PV system design variables

To date, numerous studies have examined the impacts of these variables on PVPP performance and one or more of the building energy performance metrics. For instance, Azami et al. explored the influence of building form and facade orientation on PVPP performance [4]. Similarly, Hwang et al. delved into BIPV system design variables, such as

E-mail addresses: shossei5@charlotte.edu (H. Hossei), kkim33@charlotte.edu (K.H. Kim).

^{*} Corresponding author.

Nomenclature		sDA MWh	Spatial daylight autonomy Megawatt hour
Symbols		kWh	Kilowatt hour
U Value	Heat transfer coefficient or thermal transmittance	3D	Three dimensions
α	Latitude of the location	SHGC	Solar heat gain coefficient
E	irradiance on PV surface	EPW	EnergyPlus weather file
η_{PV}	PV panels efficiency	GH	Grasshopper, a plugin for Rhino software
LF	Loss factor of the PV system	LB	Ladybug, an environmental analysis plugin for
η_{inv}	nominal rated DC-to-AC conversion efficiency of the		Grasshopper for Rhino software
	inverter	cd/m^2	Candela per cubic meter
E_{v}	Vertical illuminance	W/m	Watt per meter
L_s	Solar disc	DC	Direct current
ω_s	solid angle of the sun	AC	Alternating current
P	Position index	PVPP	PV power production
A 1.1	·	TMY	Typical meteorological year
	Abbreviations		National Solar Radiation Database
UDI	Useful daylight illuminance	CS	ClimateStudio
NZE	Net-zero energy	W/m ² K	watts per square meter per kelvin
ASHRAE	American Society of Heating, Refrigerating and Air-	c-Si	Crystalline silicon
	Conditioning Engineers	CZ	Climate zone
IGU	insulated glass unit	Tvis	Visible light transmittance
PV	Photovoltaic panel	DGP	Probability of the disturbing glare
BIPV	Building integrated photovoltaic panels	sDG	Spatial disturbing glare
WWR	Window-to-wall ratio	PVPP	PV power production
LED	Light emitting diode		

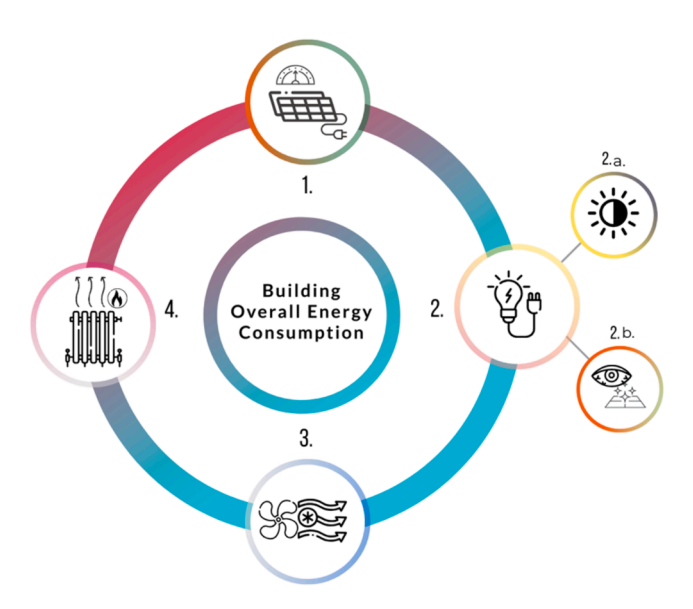


Fig. 1. Four systems' performances that affect the building's overall energy consumption: 1- pv power production, 2- lighting such as 2.a- artificial lights energy consumption and 2.b) glare, 3- cooling loads, and 4- heating loads.

module length, distance, and installation angle, affecting PV power production [5].

The orientation and tilt angle of PV modules significantly impact BIPV energy output. When PVs are installed flat on the building facade, there is an increased cosine loss compared to roof or ground-mounted PVs. Yang's research demonstrated that vertically placing PV panels on the facade reduces power output by approximately 50 % compared to the optimal angle [6]. Therefore, optimizing the panel tilt angle is crucial for achieving higher energy yield. While it has been shown that 98.6 % of the PV system's optimum performance can be achieved using a tilt angle equal to the location's latitude [7], previous studies indicate

that installing PV panels flat on the building façade generate more electricity during winter months [8,9]. Kim et al proposed a unique shape for instegrating PV into the façade of the building which had a parametric curvature to maximize the PV cells power production during the entire year [10].

[11]. Similarly, another study took into account seasonal temperatures and orientation to analyze the power production performance of different ventilated PV cladding facades in hot climate regions. The researchers concluded that regardless of the PV technology, a south-facing facade is the optimal orientation for maximizing power production. Moreover, the west and east facades generated up to 40 % more electricity from April to August. They suggested that combining the south and west facades is an effective approach to achieving nearly zero-energy buildings [12].

Alrashidi et al. demonstrated that the orientation of the PV cells affects the diurnal temrature changes of the PV cells and as a result the building cooling loads. In their experimental setup, the lower transparent PV cells caused the most reduction in the building solar heat gain [13]. Liu et al. explained that the solar irradiance levels will affect the PV panels temprature. They investigated the BIPV power performance considering PV modules material, orientation, and tilt angle [14]. Sun et al. tested application of semi-transparent window in different window-to-wall ratio (WWR) in five typical climatic zones in China. They concluded that in order to get sufficient daylight inside of the building, WWR should be 45 % or more, i.e. WWR of 75 % with 80 %transparent PV [15]. A similar study has been done by Cheng et al., assessing the performance of different WWRs in a double-glazed BIPV window. They validate the daylight simulations by experimental test. The result indicated that in order to get sufficient daylight inside of the building while reducing the building energy loads, the optimum semitransparent PV area must be 30 % or 40 % of a south-facing window with WWR 40 % [16].

1.2. BIPV power performance

To maximize the BIPV system power output various methods have been proposed in the literature. For instance, placing the PV-louvers in a

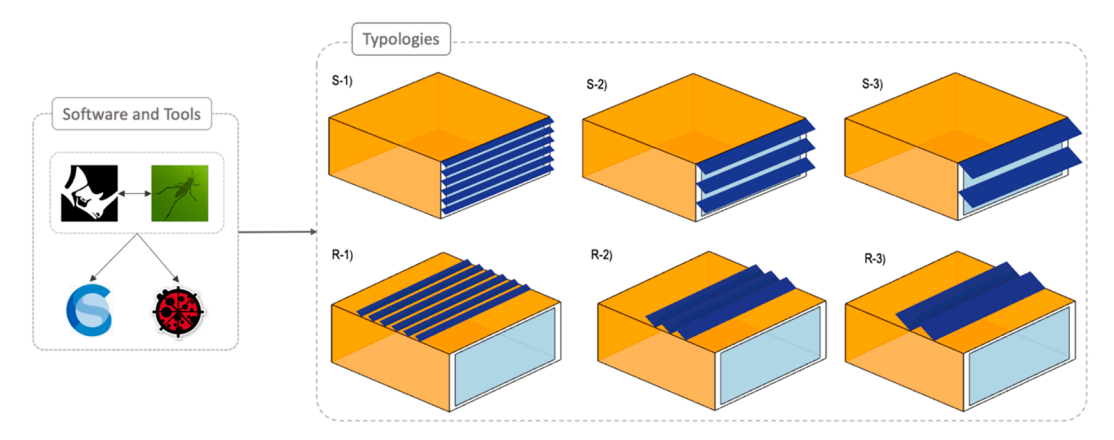


Fig. 2. Rhino and plugins including GH, CS and LB were used to simulate performances of the three PV-louvers integrated south façade and PV-mounted roof typologies.

Table 1 Locations visualization map, pv tilt angles, and climate zones list.

City, State		Climate type	Climate zone	Latitude	PV optimum tilt angle	
1	Miami, FL	Tropical	1A	25.82	24.17	
2	Houston, TX	Hot-humid	2A	29.65	26.42	
3	Phoenix, AZ	Hot-dry	2B	33.45	28.44	
4	Austin, TX	Warm-humid	3A	30.29	26.78	
5	Charlotte, NC	Warm-humid	3A	35.22	29.33	
6	Los Angeles, CA	Warm-dry	3B	33.92	28.74	
7	San Francisco, CA	Marine	3C	37.80	30.46	
8	Washington DC	Mixed-humid	4A	38.85	31.02	
9	Albuquerque, NM	Mixed-dry	4B	35.04	29.24	
10	Seattle, WA	Mixed (marine)	4C	47.53	34.57	
11	Boston, MA	Cold-humid	5A	42.37	32.53	
12	Denver, CO	Cold-dry	5B	39.83	31.45	
13	Minneapolis, MN	Cold	6A	45.07	31.45	
14	Billings, MT	Very cold	6B	45.80	33.90	
15	Fargo, ND	Subarctic	7A	46.93	34.34	
16	Gunnison, CO	Polar	7B	38.53	30.87	
17	Fairbanks, AK	Other	8	64.82	40.64	



double-skin façade and ventilating the PV panels to prevent power efficiency drop due to the temperature build-up on PV surface [17], integrating concentrated systems into the BIPV façade [18] and BIPV sun tracking systems using an irradiance model [19] to maximize the

irradiance levels reaching on the PV surface. However, in BIPVs reducing the building energy consumption is as important as increasing the PVPP. This importance is particularly amplified in BIPV facades. Therefore, architectures and designers should be well informed of

Energy & Buildings 317 (2024) 114369

Table 2Thermal properties of the opaque walls, ground floor and exterior walls in different climate zone.

Parameters		Climate Zones							
		1	2	3	4	5	6	7	8
Roof									
	U-value (W/m ² K)	0.263	0.215	0.215	0.177	0.177	0.177	0.156	0.156
	Thermal Capacity (kJ/K/m ²)	469.7	471.13	471.13	472.78	544.17	0.422	474.09	474.47
Exterior	walls								
	U-value (W/m ² K)	2.11	0.748	0.624	0.537	0.47	545.93	0.377	0.26
	Thermal Capacity (kJ/K/m ²)	532.3	538.50	540.40	542.28	544.17	545.93	547.93	556.47
Ground									
	U-value (W/m ² K)	0.806	0.729	0.703	0.692	0.584	0. 584	0.571	0.571
	Thermal Capacity (kJ/K/m²)	471.6	471.91	472.00	472.0	472.48	472.48	472.54	472.54

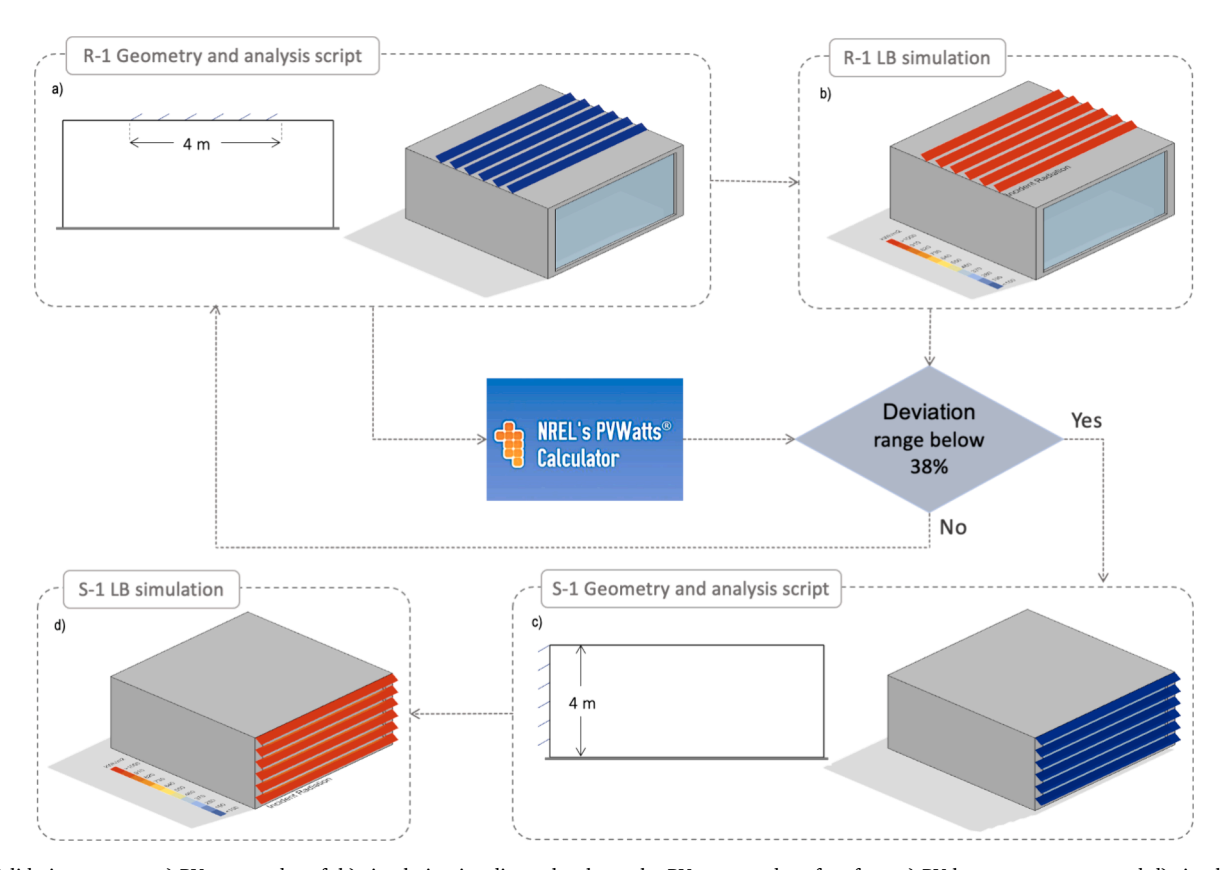


Fig. 3. Validation process. a) PV-mounted roof, b) simulating irradiance levels on the PV- mounted roof surface, c) PV-louvers geometry, and d) simulating irradiance levels on the PV-louvers surface.

consequences of each design decisions and their impact on energy performance of the building [20].

BIPV façade systems power performance has been evaluated in the literature in conjunction with either daylight performance or building energy consumption loads or both. Huang et al. simulated the performance of a PV integrated insulated glass unit (IGU) to evaluate thermal efficiency, lighting loads and PV power production for different scenarios. The results indicate that the PV IGU effectively reduced building heat gain up to 81.63 % and heat loss up to 32.03 % [21].

Shi et al. examined how various designs of PV-louvers affect cooling, heating, and lighting energy consumption across five climate types. Their findings indicate that different PV-louver designs lead to varied outcomes in building energy savings, ranging from 2.76 % to 105.74 % [22]. Kim et al. conducted experimental tests on the power production of three BIPV façades of PV-louver at a fixed angle, PV-louver installed flat on the façade, and different tilt angles of PV-blinds maximize monthly power production. They concluded that the fixed louver outperform other scenarios [23].

1.3. Impact of BIPV façade systems on building energy performance

BIPV facades attenuate solar heat and daylight penetration into the building and depending on those systems' designed components and site location, leading to varying impacts on building energy consumption. To examin their impact on heating and cooling loads, Nagy et al. suggested to integrate PV panels with overhangs to reduce unnecessary solar heat gain through windows and at the same time generating a great amount of electricity [24]. Freitas et al. compared different design arrangements of PV modules integrated in different exterior surfaces of four buildings in Brazil. Their simulations results indicate that among all of the façade application alternatives, installing PV modules as sun shading elements on the entire façade surface generates higher electricity with energy balance of up to 8.05 % of totla energy demand [2]. Cannavale et al. studied a real application of semi-transparent perovskite-based PV glazing in a building located in southern Italy. The building passive energy consumption decreased by 4 %. Net energy consumption was diminished by 15 % influenced by 27.9 MWh during a year. Comparing

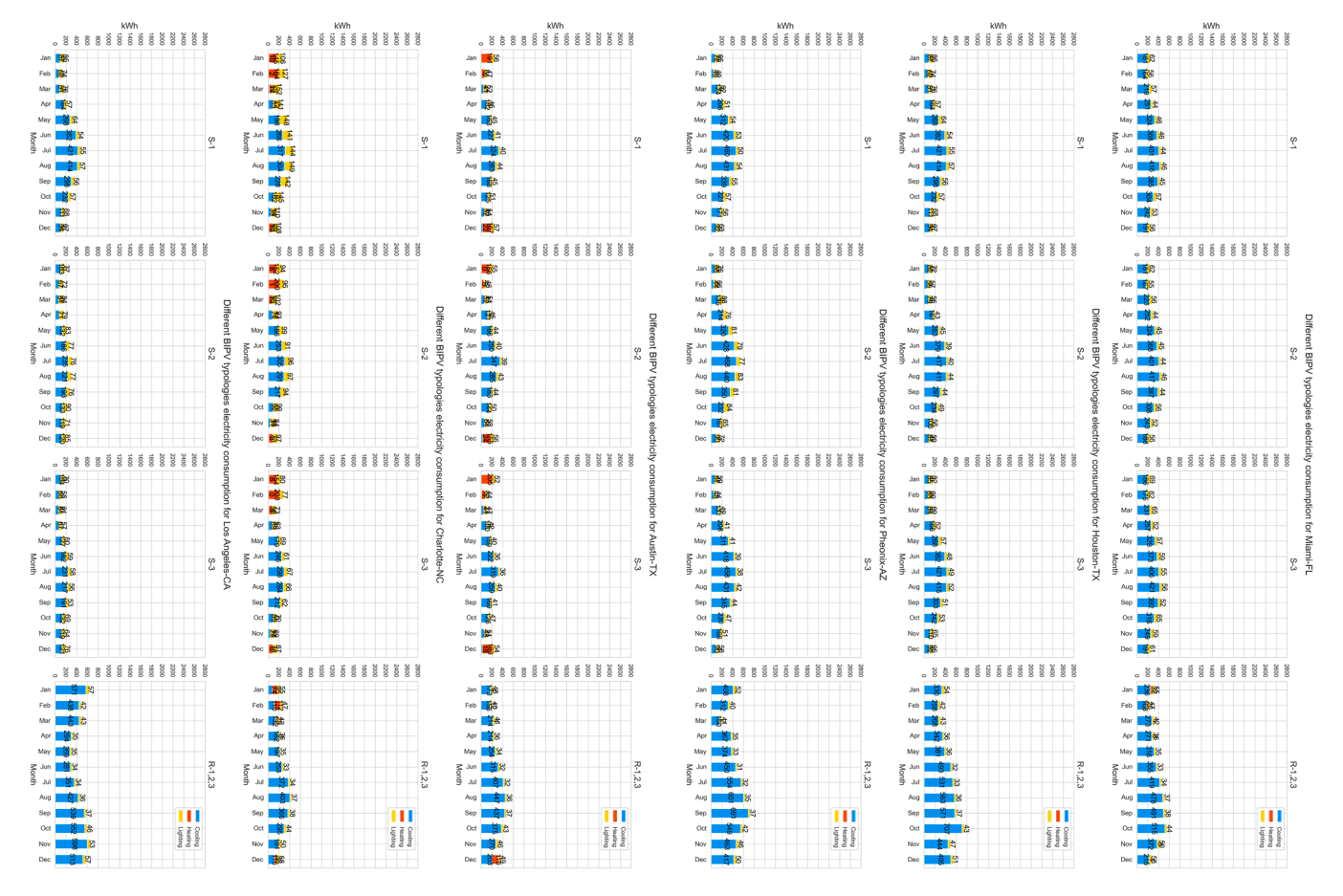


Fig. 4. Different BIPV typologies energy consumption in selected locations.

the BIPV façade and shading with regular clear glass windows, the result highlighted 18 % reduction in the overall annual electricity use of the building [25].

Olivieri et al. introduced an "energy balance index" matrix to evaluate the heating, cooling, and lighting loads, along with the annual energy performance of a single-glazed BIPV window in Madrid, Spain. Their experimentation and simulation results demonstrated that their model could achieve energy savings of at least 18 % and up to 50 % annually compared to traditional glazing windows [26]. Similarly, a study integrating PV into window blinds, considering variables such as WWR, PV material, and orientation, found that the south facade was the most advantageous for reducing net energy consumption [27].

In addition to heating and cooling performances, a number of studies also took the lighting performance into consideration. For instance, investigating energy performance of a PV vacuum glazing showed that it effectively reduced cooling loads in the climate regions with hot summer and cold winter, hot summer and warm winters, as well as heating loads in severe cold, cold and hot summer and cold winter. The energy savings potential varied based on the geographical location while it was within the range of 29.4–66.2 %. To achieve occupants' preference for illumination it was suggested to use the PV vacuum glazing in combination with the clear vacuum glass. However, for the lower latitude regions, vacuum PV glazing alone is sufficient to allow daylight penetration into the building [28].

One of the challenges of BIPV façade systems is adequate light penetration through the façade into the building. The low daylight factor inside the building will increase electricity demand to meet the indoor light requirements and occupants' optical comfort. This challenge grows in importance in monocrystalline solar cells compared to

thin PV film materials. Therefore, it is essential to ensure that the BIPV monocrystalline façade systems allow sufficient light dissemination into the building.

Riaz et al. studied the impact of a semi-transparent BIPV facade on indoor daylighting. Their experimental tests revealed an annual electricity generation of 6070 kWh alongside daylight levels in the building measuring 500 lx, and an average of 300–500 lx until 1 pm and 2:30 pm respectively during a typical day [29]. Similarly, another study examined the use of 77 % transparent PV cells on an office building facade. The results indicated that, for an office space measuring 76 m2, a combination of 8 52 W LEDs provided 676 lx. It was observed that energy consumption in the office significantly increased on cloudy days, although the researchers did not provide specific information related to the reduction factor [30].

Roberts et al investigated the effect of a semi-transparent PV-integrated double-skin facade on indoor lights. The results of the study demonstrated that the lux levels were significantly dropped in the work surface level at the center of the office room and they concluded that this type of window is not suitable for geographic locations or climate conditions similar to London, UK [31]. Compared to PV-integrated glass typologies, the BIPV blinds allow more flexibility to balance the visual effects of the façade design (Yu et al. 2021). The spacing between louvers has a greater effect on indoor light penetration in comparison to the tilt angle [32].

Assessing the potential increase in the demand for artificial lighting in occupants' working areas during daylight hours helps balance BIPV facade power production and grid electricity consumption. Various comfort lighting thresholds have been presented in the literature, including a minimum of 500 lx [28], 300 lx [33,34], and 450–600 lx for

Energy & Buildings 317 (2024) 114369

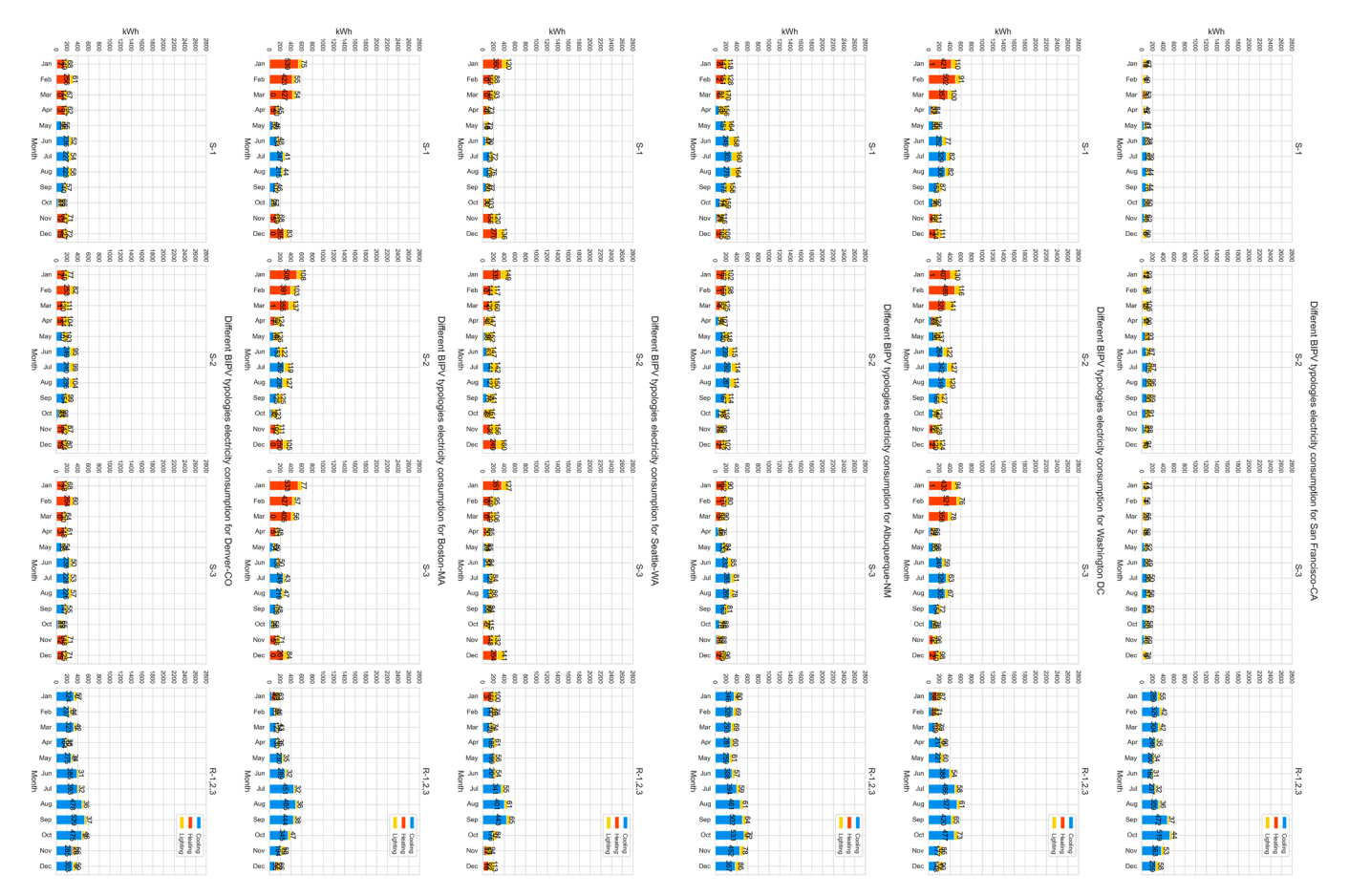


Fig. 4. (continued).

tasks such as reading, writing and typing [30]. According to the American Society of Heating, Refrigerating and Air-Conditioning Engineers (ASHRAE) indoor lighting standard, the minimum lux levels range from 30 to 50 foot-candles for open offices which is equal to approximately 300–500 lx [35]. The European Committee for Standardization suggests three baseline including 300, 500 and 750 lx for indoor illumination levels [36].

According to ASHRAE standards, spatial daylight autonomy (sDA) indicates the percentage of daylight in an occupied space during the portion of the year when the building is operating according to schedules [35]. The sDA index does not account for potential glare. Nabil et al. introduced useful daylight illuminance (UDI), which is a modified index based on sDA. Their research demonstrated that the minimum lux level required for office tasks is 500 lx, while daylight illuminance exceeding 2000 lx may cause glare [37]. Both sDA and UDI are established considering the use of indoor shutters or adjustable blinds, allowing occupants to adjust them based on the amount of daylight passing through the windows. However, achieving optimal lighting performance with BIPV facades requires considering the fixed position of the PV system on the glazing facade.

A new index for evaluating the PV-integrated windows' louvers daylighting was proposed in previous research. That means the indoor area ratio where the indoor illuminance meets 450–2000 lx and the natural light time surpasses 50 % during a month [32]. Evaluating the possibility of increasing the need for artificial lighting in occupants' working areas during daylight hours helps to balance out BIPV facades' power production and grid electricity consumption.

1.4. BIPV implementation costs

The convergence of declining PV costs and favorable energy market

conditions is creating a compelling economic case for solar installations [38]. The costs of c-Si curtainwall BIPV systems fell within the range of regular façade systems [39], making BIPV façade systems more cost friendly and affordable for many building owners. Field observation of the BIPV systems revealed that enhanced integration between PV material and the building system such as building enclosures further reduced the costs of the BIPV systems [40]. While PV modules take 43 % to 77 % of the entire system cost, with more technology advancement in PV materials efficiency and price reduction [41], the BIPV systems become more affordable for building owners.

1.5. Gap and problem statement

With the advancements in solar energy and the increasing demand to supply the building sector with renewable energies, the importance of optimizing BIPV systems to meet design requirements and occupants' comfort is becoming more significant. BIPV system implementation is on the rise due to several factors. The affordability of PV materials, which are comparable in cost to building materials, along with high land expenses for ground-mounted PV systems and power loss through transmission lines from remote solar farms, combined with rising building sale prices and the desire to enhance business image and branding, are motivating building owners and the construction industry to integrate PV systems directly into buildings rather than depending on solar farms.

Integrating PV systems into new construction is growing globally. The European Parliament has passed legislation mandating member states to install solar panels on buildings and undertake renovations to enhance energy efficiency [42,43]. Germany is leading solar implementation in Europe, with cities like Berlin, Hamburg, Rhineland-Palatinate, Bavaria, Schleswig-Holstein, and Lower Saxony having laws mandating PV system integration into buildings [44]. Similarly, in

Energy & Buildings 317 (2024) 114369

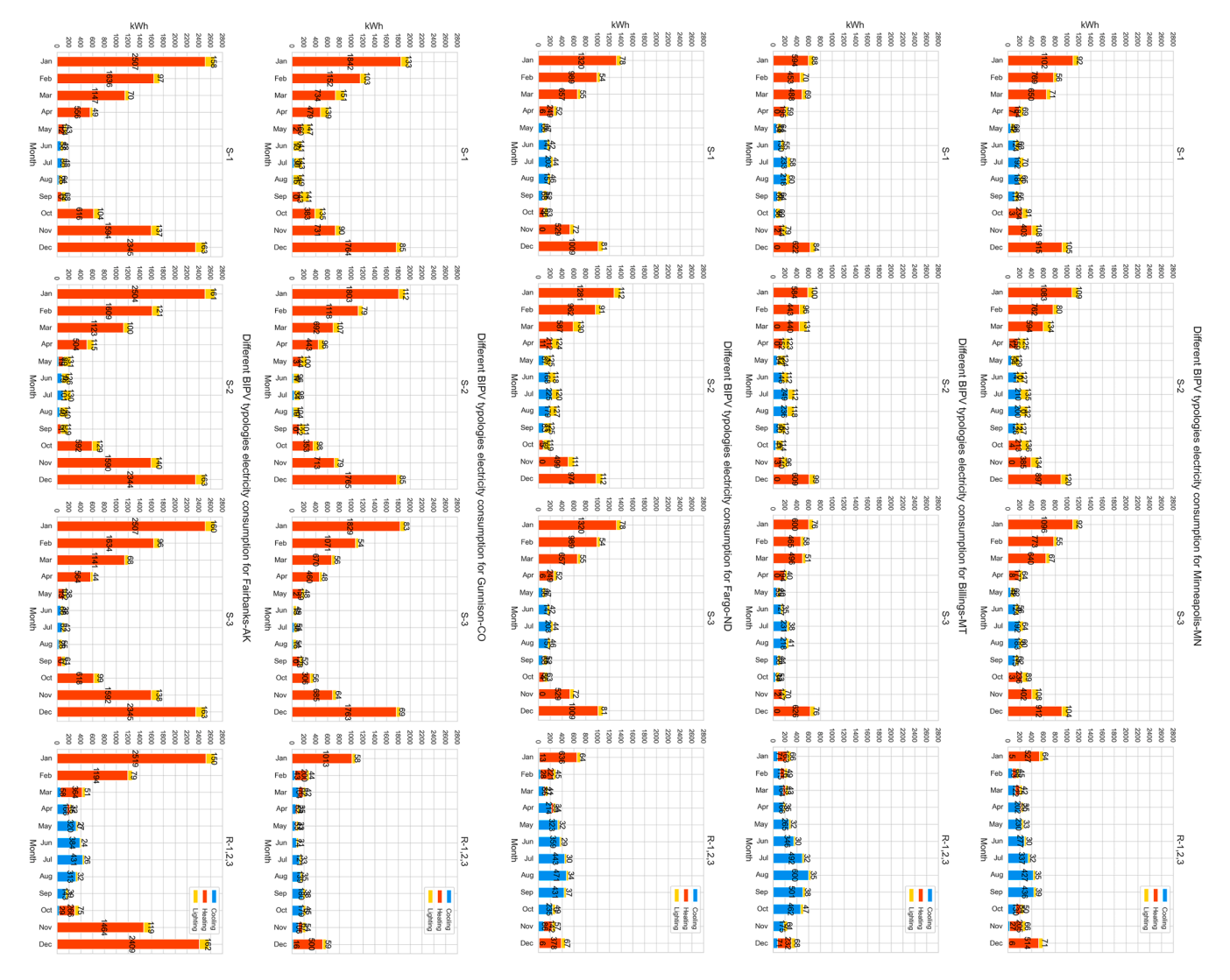


Fig. 4. (continued).

the U.S., California made rooftop solar PV a requirement on newly built homes, with some cities extending this rule to major renovations [45]. Although energy and building codes require PV integration into buildings, maximizing environmental and financial benefits of these systems requires careful planning. Solely supplying buildings with electricity from PV systems without optimizing building energy consumption is inefficient. In many cases individuals that are involved in the decision making process are uncertain whether rooftop application or facade integration will maximize power production cost savings [46]. Balancing PV power production with building energy consumption is another challenge in the design process of BIPVs, compounded by building location climate type and design constraints, which add complexity to the decision-making process. In addition to that, with urban area development and population growth, many high-rise buildings will be unable to supply the entire building with rooftop solar electricity, deterring the construction of high-rise NZE buildings. Therefore, understanding how the building's location and choosing the right BIPV components, like PV panel size, design, and installation orientation on the building's exterior, impact BIPV power production and building energy consumption is essential.

Although a review of net zero energy buildings in hot and humid climates revealed that not all the NZE buildings have blinds or shades to control glare [47], integrating PV panels into the buildings is a great way to offset grid electricity consumption specially for tall buildings [48].

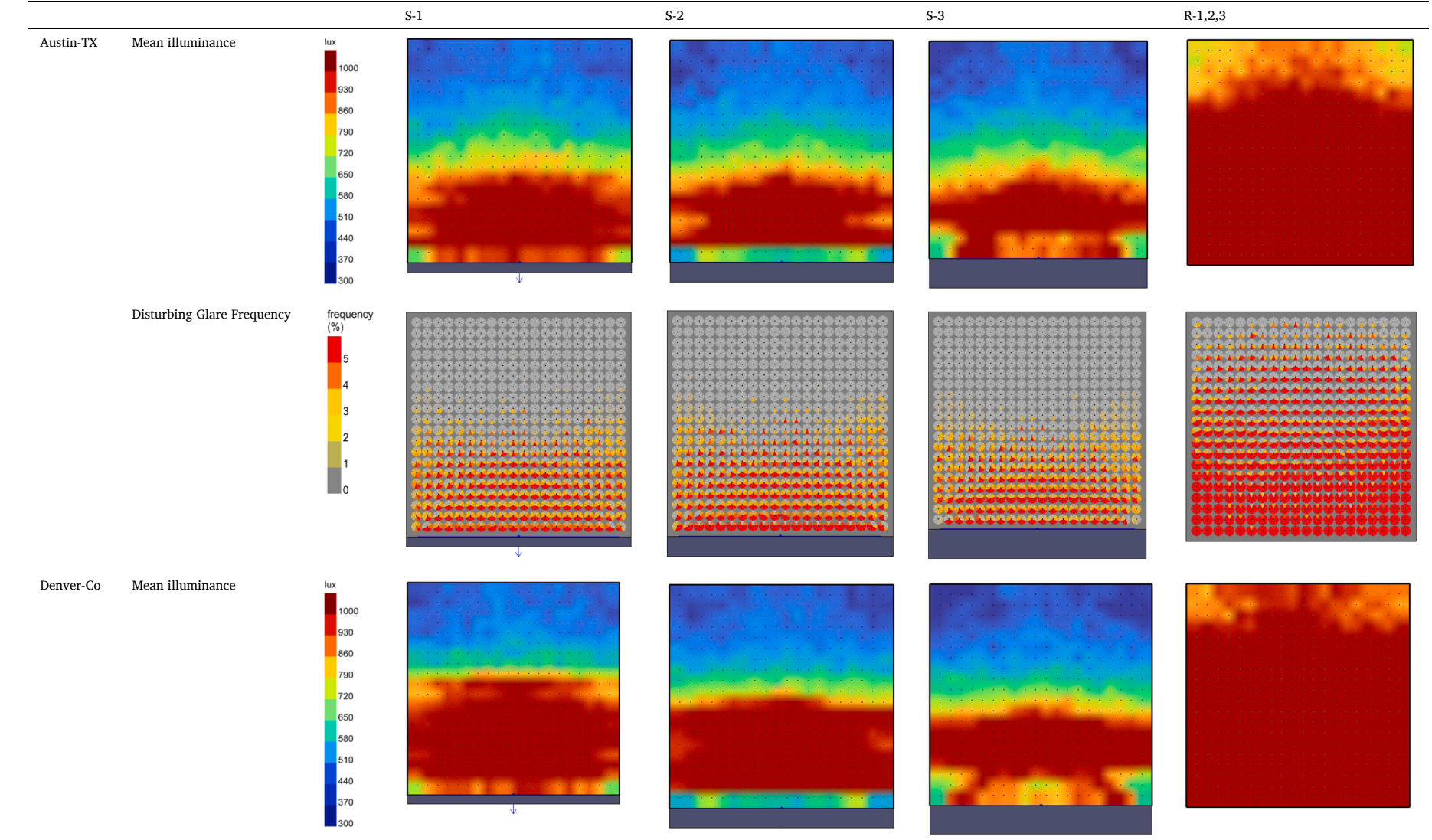
Several researchers have focused on integrating PV panels into building facades as shading devices [49] such as PV-blinds [19,50] and PV-louvers [51,52] aiming to reduce the building energy consumption while generating on-site electricity. However, studies have also investigated BIPV system performance in various climates, including hot [13], cold [53], tropical [54] and subtropical regions [55]. Nevertheless, these investigations often lacked coverage across different climate zones. For instance, studies like that of Sun et al. [15], which examined BIPV facade performance in five climate regions—severe cold, cold, temperate, hot summer cold winter, and hot summer warm winter—did not consider shading components such as louvers and blinds, as their BIPV system was flat on the facade surface.

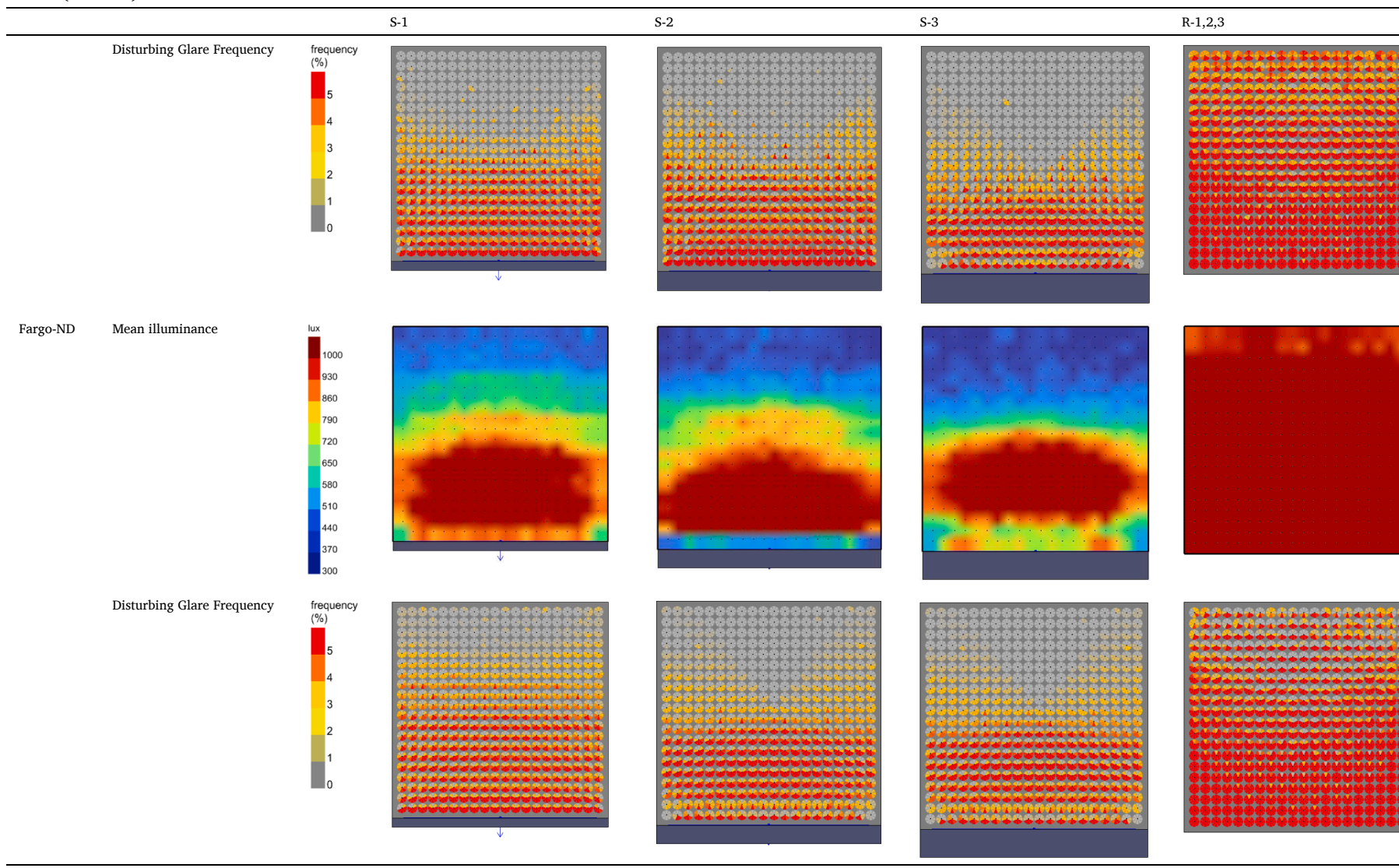
Previous research on the impact of BIPV systems on energy savings and power generation has primarily focused on individual climate zones. This study, however, utilizes a more granular breakdown of 17 locations across 16 ASHRAE climate zones [56], as defined by ASHRAE 90.1. This finer-grained approach reflects the reality that building energy code requirements for calculating energy consumption vary significantly depending on climate. By simulating energy use patterns and power production potential with this level of detail, the study allows for a more precise cross-comparison of BIPV performance across diverse climatic conditions. This approach addresses a critical gap in the existing research, where a comprehensive assessment of PV-louvers' impact on power generation and building energy consumption across all ASHRAE

(continued on next page)

 Table 3

 Mean illuminance and disturbing glare on the office working surface across different typologies in variouse latitude levels.





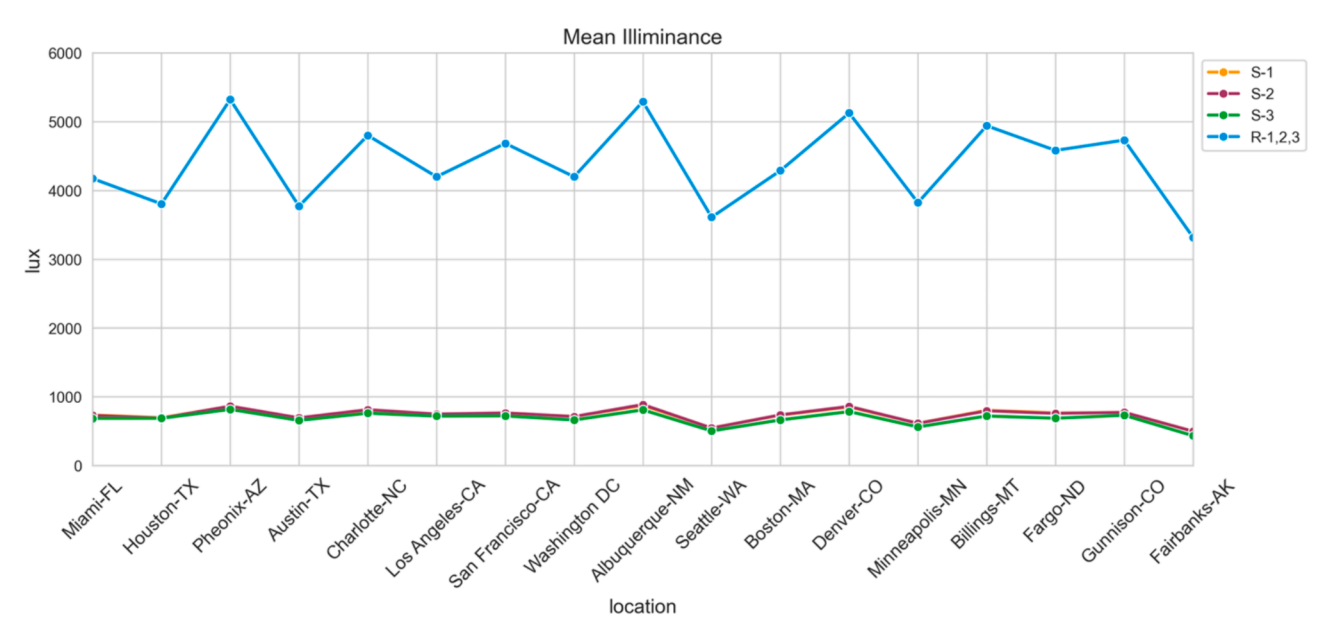


Fig. 5. Annual mean illuminance levels on office working surface.

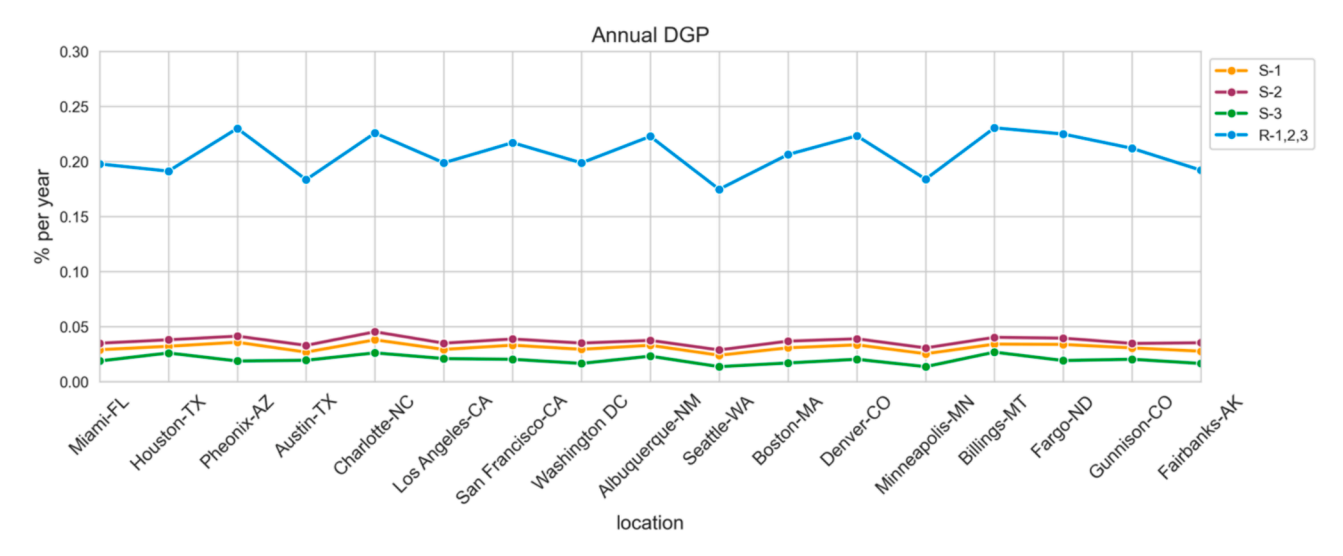


Fig. 6. Annual GDP levels on office working surface.

climate zones has been absent. To fill this gap, the study investigates the power performance and energy consumption of south-facing PV-louvers in 17 locations, utilizing three different south facade design typologies.

The outcomes of this research will provide valuable insights for homeowners, business owners, building developers, and construction professionals, enabling them to better understand how their BIPV building will perform in the real world. Additionally, this study will provide information on whether south PV-louvers will have adverse effects on building energy consumption in specific climate regions, thus assisting in informed decision-making. The results of the building energy consumption simulations and potential PVPP of this study were strongly agreed with the data from previous work done by Goia et al [57] and PVWatts [58], respectively.

2. Materials and methods

2.1. Geometry

To conduct the simulations, a single room with dimensions of $10\ m\ x$ $10\ m\ x$ $4\ m$ (length, depth and height) was model in Rhino a 3D

modeling software [59]. Each typology included a south-facing window with a window-to-wall ratio (WWR) of 80 %. Rooms with a high fenestration ratio often experience overheating, resulting in discomfort or increased energy consumption, even in colder climates [60]. However, to isolate the impact of BIPV systems on building performance and highlight the differences, the rooftop typologies were considered without any shading on the south window, excluding the influence of non-BIPV parameters.

The overall simulation workflow included six BIPV typologies, three typologies of PV-louvers on the south glass facade and three roof-mounted PV (Fig. 2). While maintaining a consistent total surface area of 30 m 2 for the PV system, the depth and number of PV-louvers differed across various typologies: in S-1 and R-1, there were 6 louvers at a depth of 0.5 m; in S-2 and R-2, there were 3 louvers at a depth of 1 m; and in S-3 and R-3, there were 2 louvers at a depth of 1.5 m.

2.2. Site condition and building zone setup

To analyze the performance of this model in various locations, a combination of seamlessly integrated software tools was utilized.

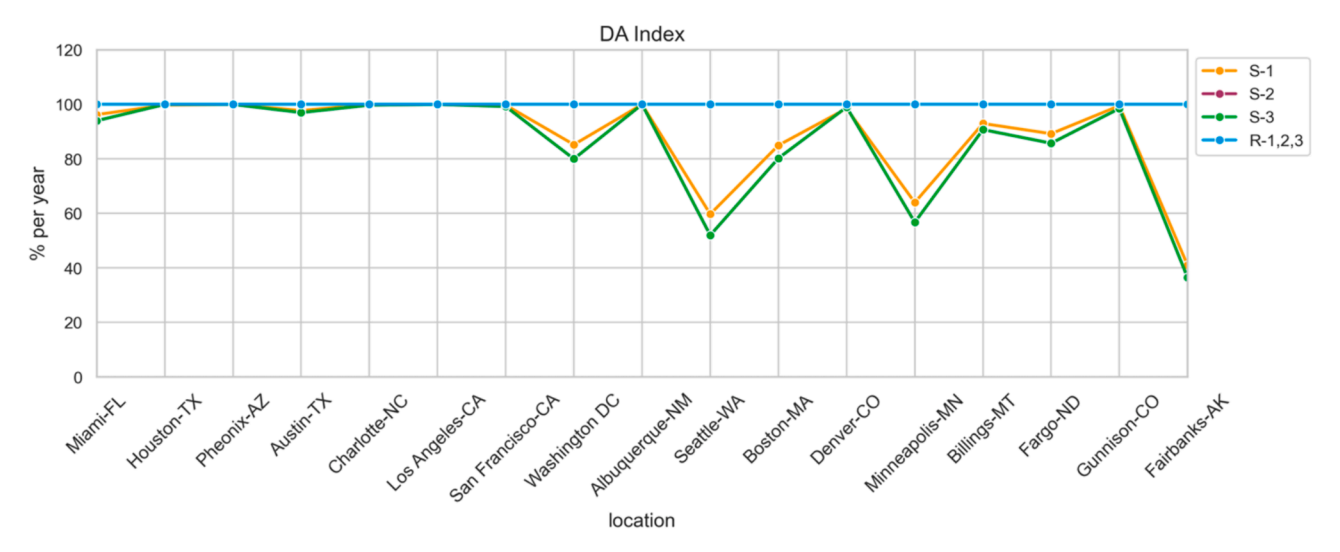


Fig. 7. DA index in various locations.

Grasshopper (GH), a visual programming environment tightly integrated with Rhino, provided a streamlined workflow for defining and running the simulations [59]. Ladybug (LB version 1.7.0) tools act as a bridge, connecting Rhino's 3D modeling capabilities to a range of validated simulation engines [61]. In this study, LB utilized EnergyPlus engine [62] along with EnergyPlus Weather (EPW) data [63] for simulating irradiance levels on the PV panels. Finally, ClimateStudio [64] (CS version 1.9.8), a plugin for Rhino that built on Radiance and EnergyPlus engines, was used to simulate the building's lighting, heating, and cooling loads.

The building energy performance analysis was conducted in 17 different locations in the U.S., across various climate regions (Table 1). Building program was set to an open medium office. ASHRAE 90.1 were used as the building standards in all the energy simulation settings. In all simulation runs, the building program was configured for a medium open-space office, and occupancy schedules were adjusted to match typical office operations. Weekdays began at 6 am and gradually ramped up until fully occupied by 9 am, then started decreasing at 3 pm until reaching vacancy at 9 pm. On the first day of the weekend, operations began at 6 am, increased to half occupancy by midday, and then decreased starting at 2 pm until fully vacant by 5 pm. The second day of the weekend had no occupancy scheduled.

2.3. BIPV system potential power production

The optimum tilt angle of the PV modules in both PV-louvers and roof-mounted PV typologies were calculated using equation (1) from Jacobson et al. research [65].

$$1.3793 + \alpha \times (1.2011 + \alpha \times (-0.014404 + \alpha \times (0.000080509)))$$
 (1)

where α is the latitude of the location.

The LB plug-in utilizes the EnergyPlus code to define sky matrix attributes based on the analysis period and the location weather data. In this part of the analysis workflow, the Cumulative Sky Matrix component was used to create a matrix of both direct normal radiation and diffuse horizontal radiation values from each path of sky dome. The analysis period was set to one month to calculate the average daily irradiance levels (kWh/m2/day) on the PV surface for each month. Nonuniform irradiance levels are a common issue in PV-louver systems due to self-shading of panels. This leads to a significant voltage drop, resulting in a dramatic reduction in PVPP performance. Previous research [48] proposed a new circuit connection for partially shaded BIPV systems. According to their study, a hybrid connection of series and parallel connections between the cells mitigated the voltage drop from

98 % to 21 %. Since LB simulates the irradiance levels falling on the PV surface, incorporating this hybrid circuit connection approach could potentially convert a majority of the received irradiance into power. Therefore, the calculation of potential power production for the PV system in this study relies on the irradiance levels, demonstrated in equation (2).

$$PVPP = E \times \eta_{PV} \times (1 - LF) \times \eta_{inv}$$
 (2)

Where

PVPP is potential power production,

E is irradiance on PV surface,

 η_{PV} is PV panels efficiency,

LF is loss factor.

 η_{inv} is nominal rated DC-to-AC conversion efficiency of the inverter. Mono crystalline silicon (c-Si) PV cells were considered for the PV material in all typologies. While in the laboratory conditions c-Si PVs have an efficiency range of 25 %-27 %, their real-world efficiency varies from 16 % to 22 % [66]. In this study, η_{PV} considered to be 19 % which is the median of the real-world c-Si PV efficiency range. For LF factor, losses due to soiling, shading, snow, mismatch, wiring, connector, light-induced degradation, nameplate rating, age, and availability, were accounted for 14.08 % [67]. The η_{inv} factor established by the National Renewable Energy Lab (NREL), is considered to be 96 % [67].

The simulated potential rooftop typologies' PVPP were validated by PVWatts (version 8) [58] which is an online simulation tool used for modeling and predicting the performance of grid-connected PV systems, including rooftop installations. It relies on an hourly typical meteorological year (TMY) database from the National Solar Radiation Database (NSRDB) and considers factors like location, system size, tilt angle, azimuth, and solar radiation data. Given that PVWatts has been shown to underestimate PV system potential power generation by up to 38 % [68], our study reveals that the simulated power outputs of various roof typologies exhibited deviations ranging from 4 % to 28 % compared to the PVWatts calculator. Despite these variances, there was a clear alignment in the trend of PV potential power production between our simulations and the PVWatts data. After verifying the accuracy of the simulation script with the PVWatts data output, the PV array was repositioned from the horizontal roof surface to the vertical south facade surface for simulating the PV-louvers potential PVPP (Fig. 3).

2.3.1. Building energy consumption

In this simulation workflow, the PV-louvers were defined as shading devices while the roof-mounted PV typologies had no shades on the south façade glazing area. A double-glazing system with 6 mm glass, 6

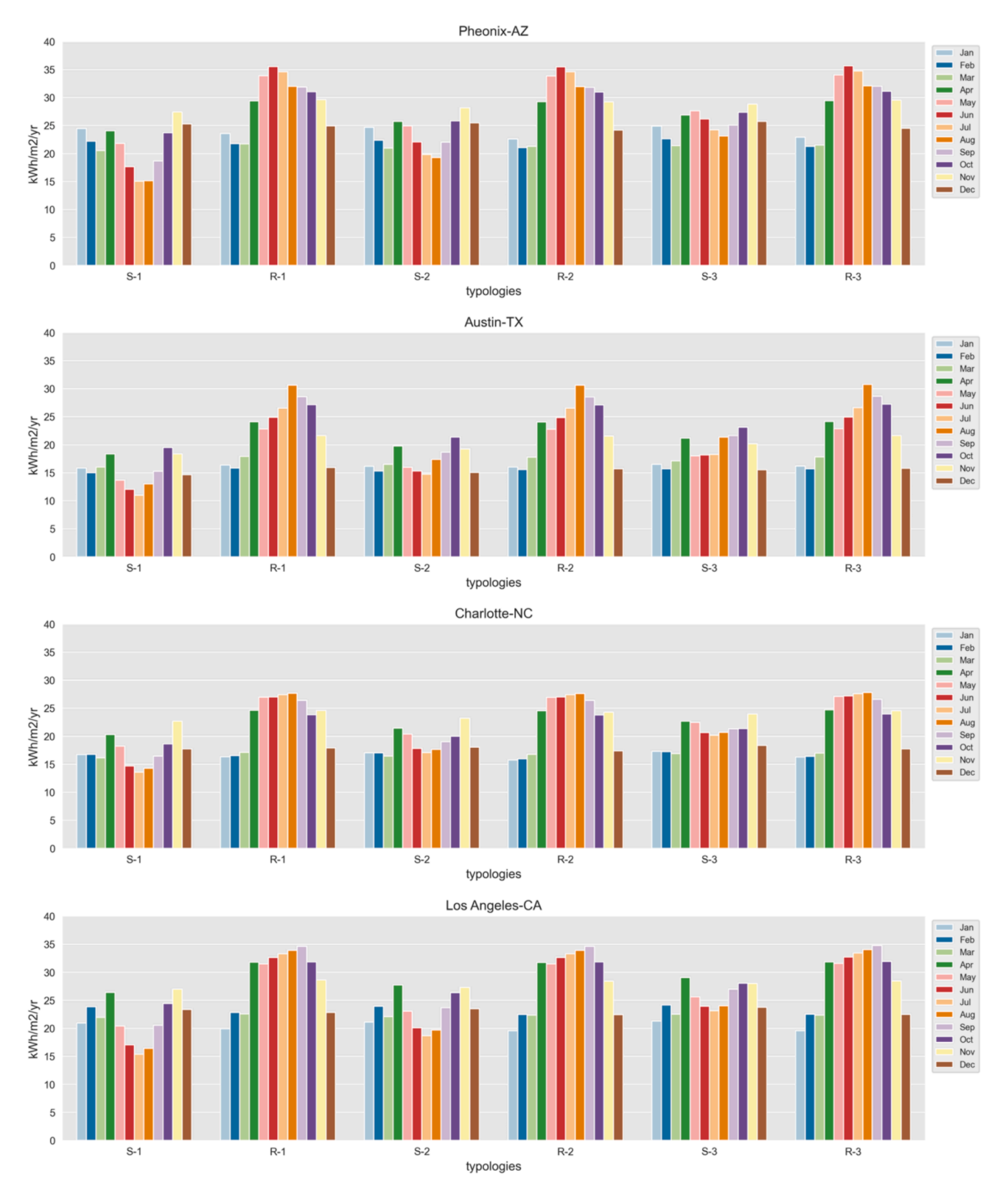


Fig. 8. Power production of different typologies in selected locations.

mm air gap was considered in all typologies and locations. U-value (W/m^2K), SHGC and Tvis of the window were set to 2.67, 0.703 and 0.781, respectively. Thermal properties of the opaque walls, roof and floor surfaces of the building were set to align with current standards requirements and contemporary recommendations in each locations' climate zone (see Table 2). The heating (E_H), cooling (E_C) and lighting

(E_L) loads of the room were simulated in all building typologies using CS.

The accuracy of the energy consumption simulation script for an 80 % WWR was validated by comparing the energy consumption of the roof typologies with data from previous research [57]. Afterwards, energy performance of the PV-louvers on the south-facing facade was analyzed and compared to their respective roof designs, assuming a grid

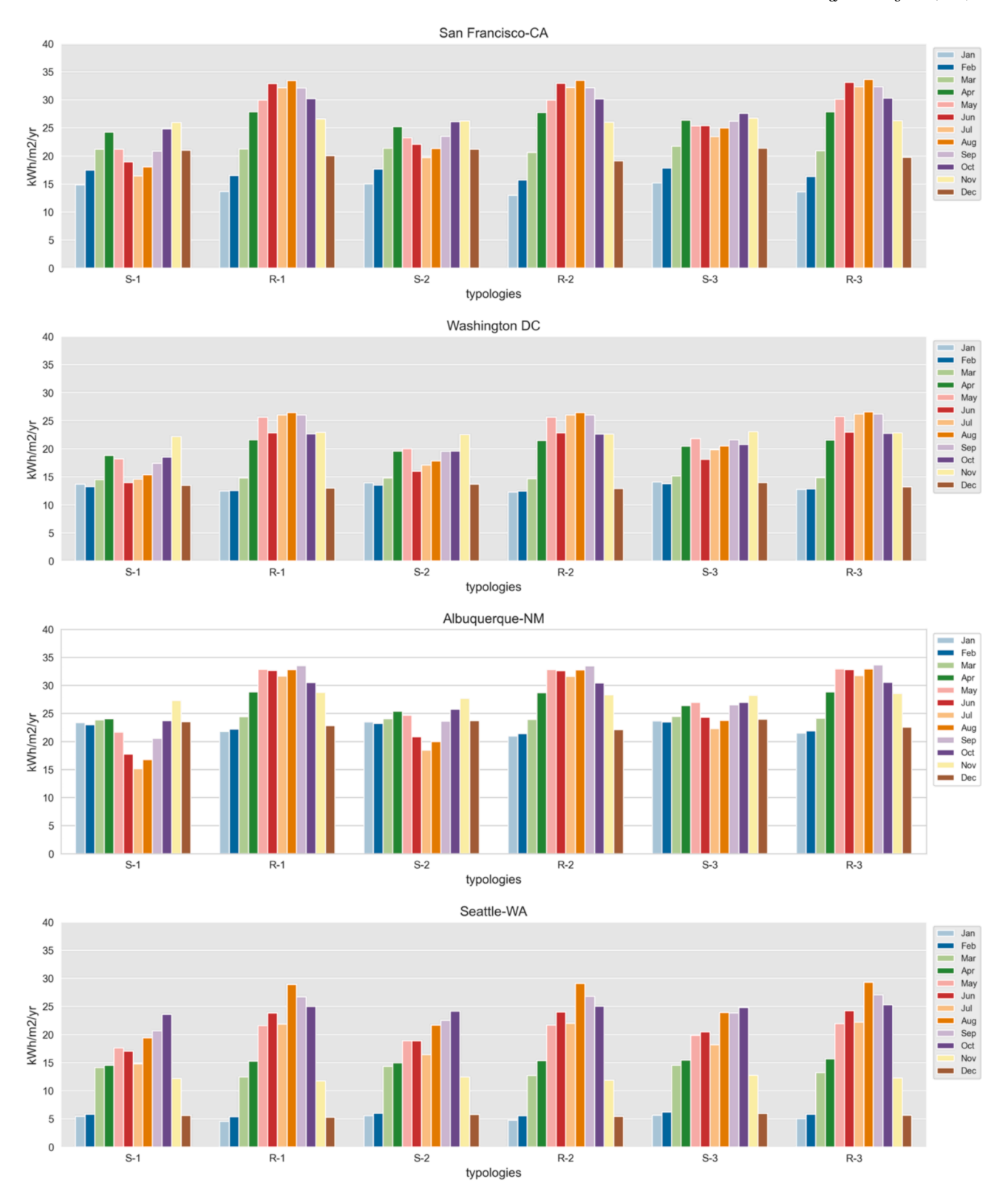


Fig. 8. (continued).

connection without energy storage. The net energy use was calculated by subtracting power generated by PV system (E_{PV}) from sum of the loads using the equation below:

$$E_{net} = E_H + E_C + E_L - E_{PV} \tag{3}$$

Lighting availability schedules were set to the office schedule with the

power density of 6.5 W/m. The working surface height for daylight and glare analysis was set at $0.75\,\mathrm{m}$ above the floor. An array of 400 sensory grid points on the working surface calculated the daylight and glare simulations among all typologies. The assigned material to each geometry surfaces had a diffuse factor of 70 %, 50 % and 20 % for ceiling, walls and floor, respectively. The acceptable illuminance levels range

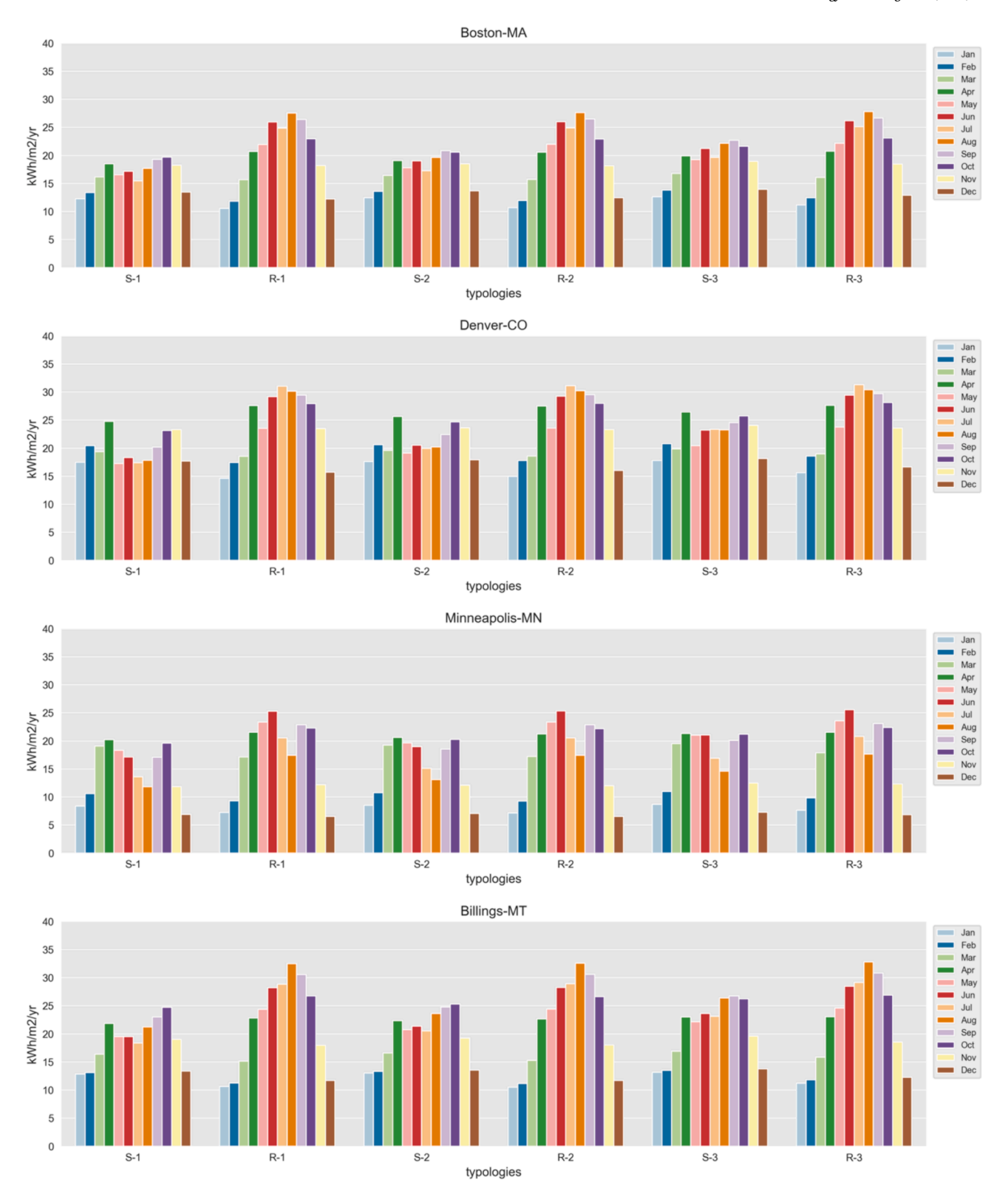


Fig. 8. (continued).

were defined 300 lx to 1000 lx, according to IES Lighting Standards $\[[69]]$.

2.3.2. Occupants visual comfort

Occupants visual comfort was assessed by simulating the probability of the disturbing glare (DGP) and mean illuminance levels on the working surface.

The CS uses the Radiance ray tracer to calculate the distribution of illuminance, determining the probability of disruptive glare when light levels exceed 320 lx across eight distinct viewing angles.

$$DGP = c_1 \times E_v + c_2 \times log \left(1 + \sum_{i} \frac{L_{s,i}^2 \times \omega_{s,i}}{E_v^{a_1} \times P_i^2} \right) + c_3$$
 (4)

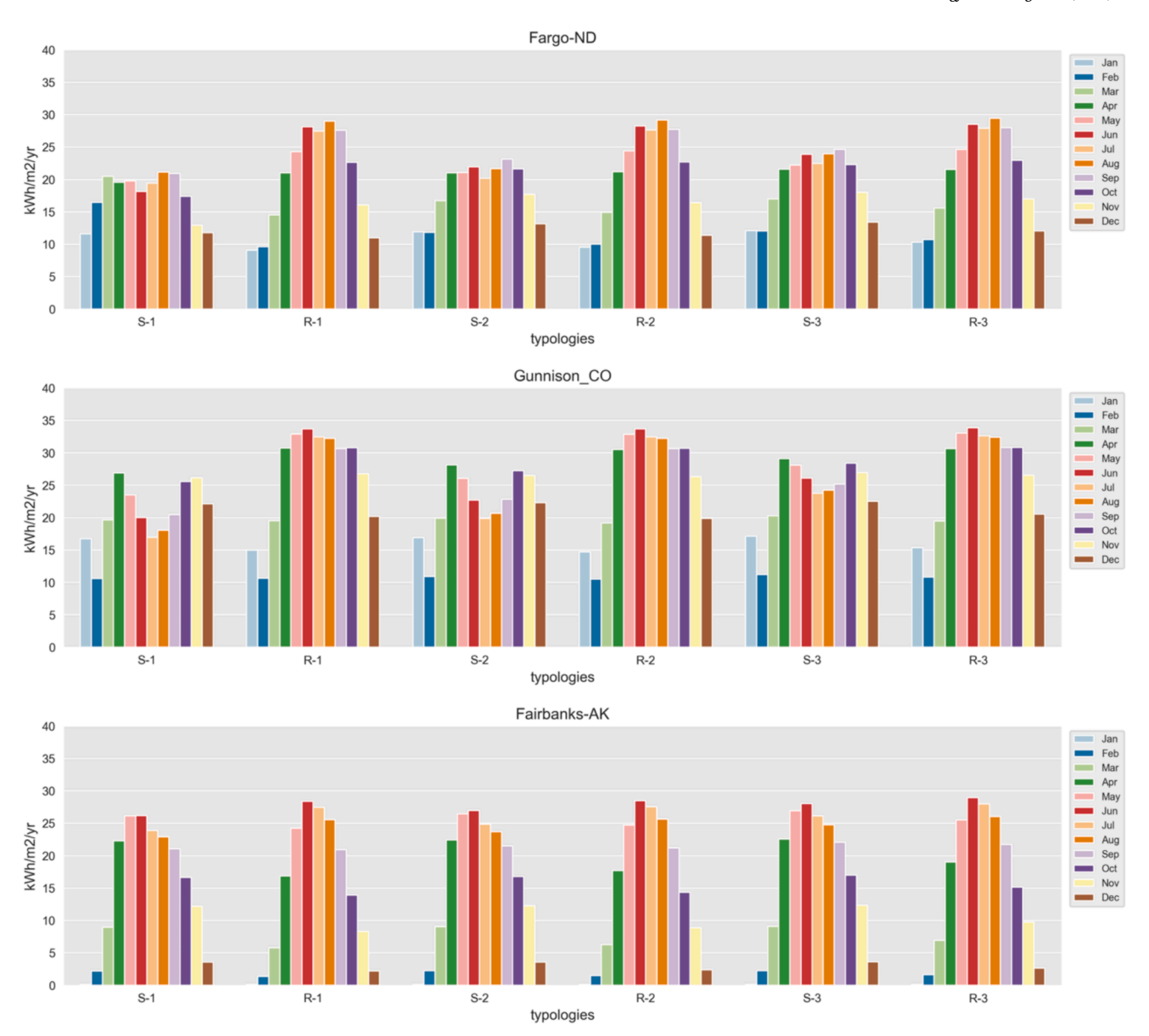


Fig. 8. (continued).

where

 E_{v} is vertical illuminance (lux),

 L_s is solar disc (cd/m²),

 ω_{s} is solid angle of the sun,

P is position index.

Based on simulation results, the CS classifies DGP into four ranges: DGP \leq 34% as imperceptible glare, 34% < DGP \leq 38% as perceptible glare, 38% < DGP \leq 45% as disturbing glare, and DGP > 45% as intolerable glare. This study focuses on spatial disturbing glare (sDG) to assess visual comfort in BIPV typologies. sDG values signify views across the occupied floor area experiencing disturbing or intolerable Glare (DGP > 38%) for at least 5% of occupied hours.

3. Results

The heating, cooling and lighting energy consumption of 6 different BIPV systems were simulated in 17 different U.S. locations across all ASHRAE climate zones. Fig. 4 depicts the results of thermal and lighting loads. The impact of adding PV-louvers to the south glass facade varied across different climate zones in terms of the building's annual cooling

and heating loads. Interestingly, in tropical climates, the effect on reducing cooling loads was minimal. However, in hot-humid, hot-dry, warm-humid, warm-dry, and marine climates, the reduction in heating loads increased, with the most significant reduction observed in San Francisco, CA, which falls under the marine climate zone. In mixed-humid, mixed-dry, and mixed (marine) climate zones, PV-louvers decreased cooling loads but led to an increase in heating loads. Nevertheless, the total thermal electricity loads for the buildings remained relatively consistent after integrating the PV-louvers on the south window. Although PV-louvers resulted in a reduction of cooling loads in cold-humid, cold-dry, cold, and very cold climate regions, they significantly increased heating loads, especially from cold-humid to very cold climates. The decrease in cooling loads in subarctic, polar, and "other" climate regions was minor, while the increase in heating loads was dramatic.

Roof typologies allowed more daylight through the south window, however as shown in Fig. 4, BIPV façade typologies consumed more electricity to meet standard lighting levels for offices. Nevertheless, the mean illuminance levels on the office work surface exceeded standard thresholds in roof typologies, leading to excessive glare for at least half of the floor area. Table 3 presents visualized mean illuminance levels

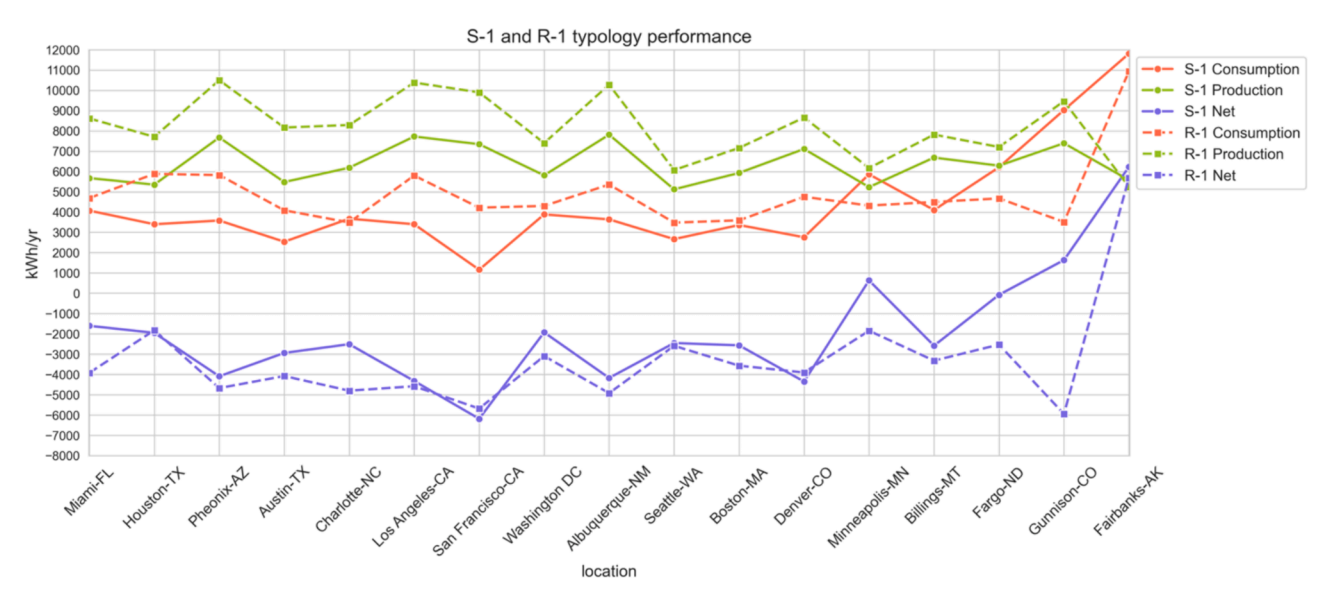


Fig. 9. S-1 and R-1 typologies electricity production, consumption and net.

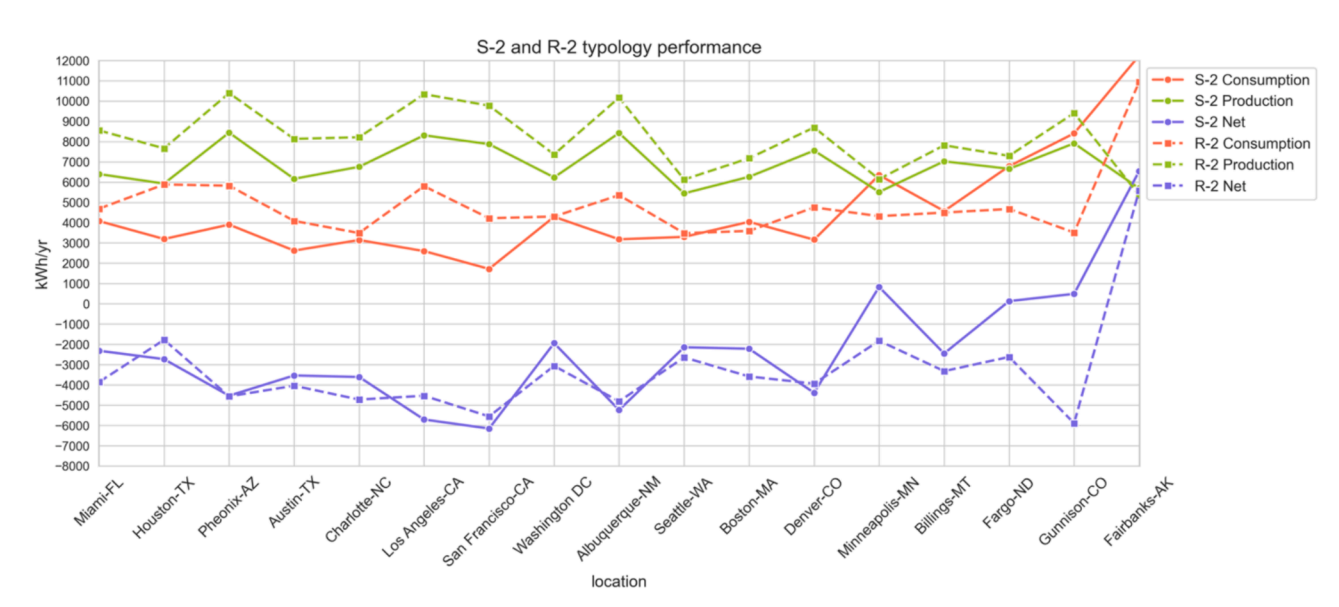


Fig. 10. S-2 and R-2 typologies electricity production, consumption and net.

and evidence of disturbing glare in three locations: Austin, TX; Denver, CO; and Fargo, ND. The frequency of this distracting glare increased with the location's latitude, from Austin (30.29° N) to Fargo, ND (46.93° N). As Fig. 5 depicts, the mean illuminance levels of the roof typologies exceed the standard threshold of 2000 lx across all the locations. Fig. 6 shows the DGP for other locations. On average, roof typologies had a DGP of 20 % across different locations. Seattle, WA had the lowest DGP at 17 %, while Billings, MT had the highest at 23 %. Façade typologies significantly reduced DGP compared to roof typologies. The average DGP for S-1, S-2, and S-3 typologies was 3.0 %, 3.6 %, and 1.9 %, respectively (see Fig. 6).

The mean illuminance levels of all PV-louver typologies were within the standard range of 300 lx to 1000 lx. However, both the mean illuminance levels and the DA index experienced a steep decrease in Fairbanks, AK, which can be attributed to its high latitude and the prevailing sky and weather conditions near the North Pole. Nonetheless, the PV-louver typologies achieved a DA index of 1 or fairly close to 1 in various locations, including Miami, FL, Phoenix, AZ, Austin, TX, Los Angeles, CA, San Francisco, CA, Albuquerque, NM, Denver, CO, and

Gunnison, CO (Fig. 7).

Fig. 8 presents the monthly PV power production for each typology at each location. Comparisons between the south-facing façade typologies and their corresponding roof typologies reveal that roof typologies generally outperformed the façade BIPVs in terms of monthly power production. However, as the depth of the PV panels increased, the power output of the façade typologies progressively approached that of the roof typologies within the same category. A comparison of the monthly PV system power generation across all the typologies and locations revealed a distinct pattern (see Fig. 8).

Locations situated above 40° North latitude, including Fairbanks, AK, Fargo, ND, Billings, MT, Minneapolis, MN, Boston, MA, and Seattle, WA, typically generated less power during winter months and more power during summer months. Conversely, locations closer to the equator such as Miami, FL, Phoenix, AZ, and Austin, TX exhibited peak power production in winter months and then power production declined around month of June.

Figs. 9, 10, and 11 depict the energy consumption, production, and net values for roof and PV-louvers typologies. Building energy

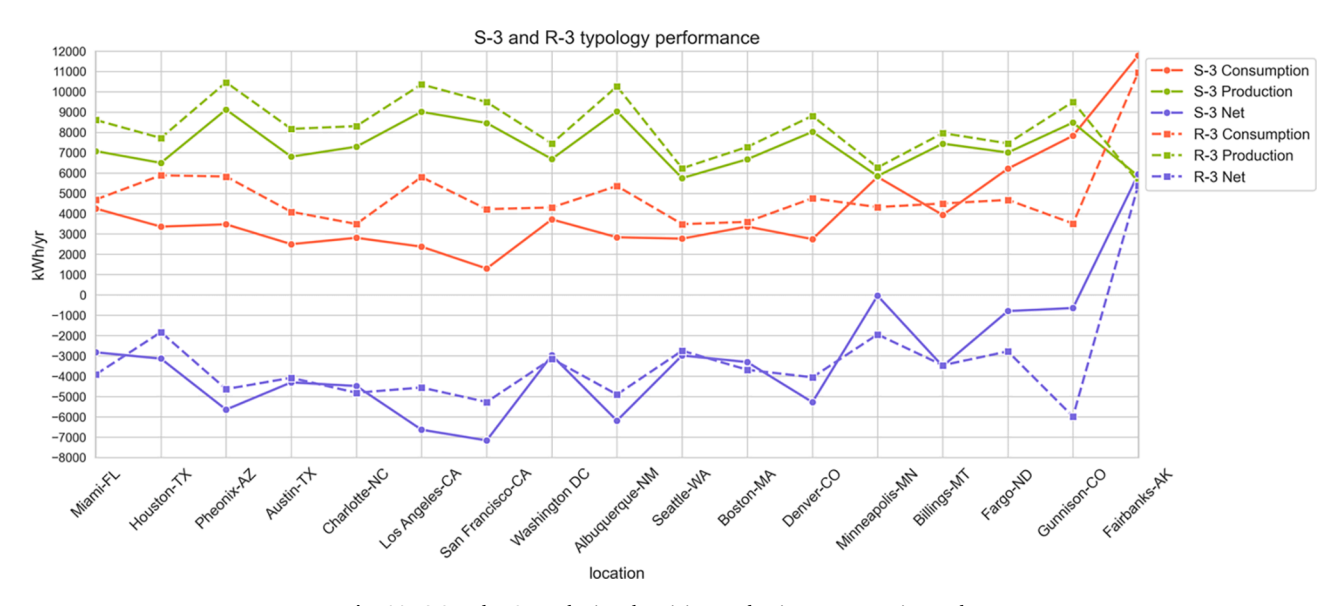


Fig. 11. S-3 and R-3 typologies electricity production, consumption and net.

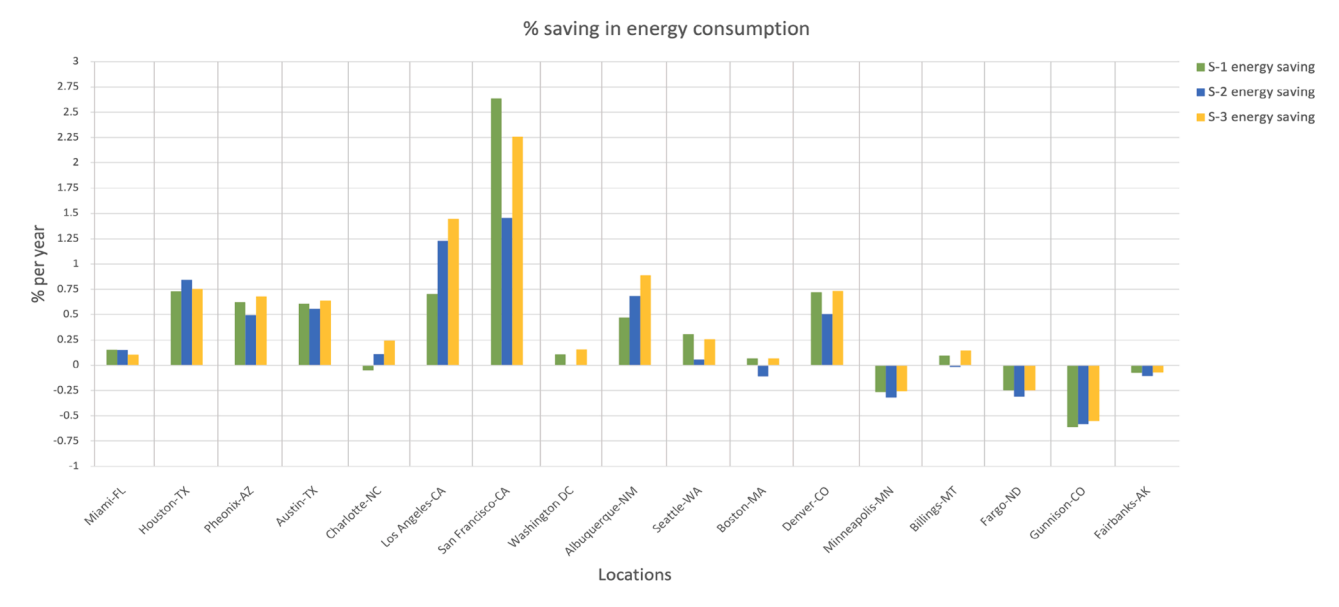


Fig. 12. Impact of integrating pv-louvers on the south façade in building energy savings.

Table 4Peak power output in each location throughout a year.

City, State	Month of peak output		
Miami, FL	November		
Houston, TX	October		
Phoenix, AZ	October		
Austin, TX	October		
Charlotte, NC	October		
Los Angeles, CA	Varied		
San Francisco, CA	September		
Washington DC	October		
Albuquerque, NM	October		
Seattle, WA	September		
Boston, MA	August		
Denver, CO	March		
Minneapolis, MN	March, September		
Billings, MT	August		
Fargo, ND	August		
Gunnison, CO	March		
Fairbanks, AK	May		

consumption of S-1, R-1 and S-2, R-2 typologies was approximately equal at Charlotte, NC, Washington DC, Boston, MA, and Billings MT. However, the S-3 façade typology displayed a slightly better performance in those locations. Except for Minneapolis, MN, the façade typologies reduced building energy consumption in all other locations (see Fig. 11).

The total building energy consumption which is the sum of cooling, heating, and lighting loads significantly declined in Gunnison, CO, because of a harsh climate, and in Fairbanks, AK, due to both a higher latitude and harsh climate. Increasing the depth of PV panels brought the power production performance closer to that of roof typologies. Additionally, in locations with mild climates like Houston, TX, Phoenix AZ, Austin, TX, Charlotte, NC, Los Angeles, CA, and San Francisco, CA, deeper PV panels in both façade and roof increased the net power output.

The S-1 typology outperformed other façade typologies in San Francesco, CA and Seattle, WA which are in climate zone 3C and 4C.

4. Conclusion

This study aims to conduct a comprehensive evaluation of the impact of south-facing PV-integrated louvers on not only potential PVPP but also building energy performance and occupants' visual comfort, including glare and mean illuminance levels. The study examined six different BIPV typologies across all ASHRAE climate regions in the U.S. The performance of PV-louvers integrated into the south facade typology is compared with the corresponding roof application to understand the effectiveness of the BIPV facade system in addressing building energy needs. The findings of this study have led to the following conclusions regarding BIPV systems in ASHRAE climate zones:

4.1. Climate zone 1

All PV-louver typologies successfully reduced building energy consumption. The percentage of energy savings was higher in S-1 and S-2 typologies compared to S-3. While the roof typologies consumed more energy, the net energy of these typologies was higher, primarily due to increased potential PVPP. Additionally, increasing the depth of the PV panels enhanced the performance of the potential PVPP and increased the net energy of the facade typologies.

4.2. Climate zone 2

Incorporating PV-louvers into the facade significantly reduced building energy consumption. Increasing the depth of the PV panels boosted PVPP from the PV-louvers, consequently raising the net energy of the S-3 typologies above that of the R-3 typology.

4.3. Climate zone 3

PV-louvers proved more effective in reducing building energy consumption in sub-climate types B and C compared to sub-climate type A. Despite lower potential PVPP in S-2 and S-3 typologies compared to roof typologies, the net energy of the facade typologies surpassed that of the roof typologies. Moreover, increasing the depth of the PV panels resulted in higher net energy for the facade typologies.

4.4. Climate zone 4

Overall, integrating the PV-louvers into the facade led to a slight reduction in building energy consumption. A direct correlation between the depth of the PV panels and the building's net energy was observed in facade typologies.

4.5. Climate zone 5

The building energy consumption remained fairly consistent after integrating PV-louvers into the facade in sub-climate type A. However, it reduced the building energy consumption in sub-climate type B. Specifically, the S-2 typology had adverse effects on building energy consumption in sub-climate type A. On the other hand, PV-louver typologies outperformed roof typologies in sub-climate type B.

4.6. Climate zone 6

The PVPP of facade typologies was fairly close to that of roof typologies, and as the depth of the panels increased, the values became even closer. However, facade typologies had an adverse effect on building energy consumption in sub-climate type A. Although the S-2 typology worsened the building energy consumption, S-1 and S-3 improved it in sub-climate type B. Furthermore, S-3 exhibited greater improvement than S-1. Overall, the net energy of the roof typologies was higher than that of the facade typologies across all typologies.

4.7. Climate zone 7

The facade typologies led to an increase in building energy consumption, with this adverse effect being more pronounced in subclimate type B. Additionally, the net energy of the roof typologies was higher.

4.8. Climate zone 8

Despite the potential PVPP of the facade and roof typologies being very close, the facade typologies had a negative effect on building energy consumption.

For further analyzing the efficacy of the façade typologies in offsetting the building electricity consumption, percentage of yearly energy savings across all locations depicted in Fig. 12. Regardless of the installation location of the PVs in each typology, PV system had a peak in monthly power generation at each location. Table 4 shows month of peak power output in each location over a year. This information will be crucial for managing the electricity generated by the PV panels throughout the year and defining the size of other components of the system such as battery storages.

All three PV-louver designs reduced sunlight penetration while achieving the required illuminance levels of 300–1000 lx across most of the floor area. Although less lighting load in roof typologies were observed, the mean illuminance levels on the working surface were on the other hand significantly high which caused disturbing glare for the occupants in a large portion of the floor area.

The applicability of BIPV louvers depends on achieving a balance between maximizing potential power generation and maintaining or improving building energy performance. This study demonstrates that while facade typologies can be effective in reducing energy consumption in some ASHRAE climate zones (1–3, 4B and 5B), they may have an adverse effect in others (6, 7, 8). This underscores the importance of considering climate data and sub-climate variations when designing BIPV louver systems. For instance, in zones with high solar radiation (1–3), deeper facade typologies offer a good balance between energy savings and power generation.

Furthermore, the applicability of BIPV louvers can be viewed through the lens of building use and design objectives. In buildings prioritizing energy savings and occupant comfort, such as office buildings, facade typologies are suitable choices in climate zones of $1{\text -}3$, 4B and 5B due to their ability to reduce cooling loads and offer shading benefits. Conversely, in buildings where maximizing power generation is the primary goal, like commercial buildings with high electricity demands, roof-mounted typologies may be more applicable across a wider range of climates, considering their generally higher potential power generation observed in this study.

While the impact of building height on energy production with BIPV louvers is not directly addressed in this study, the results suggest that facade typologies can be more competitive with roof-mounted systems in taller buildings. This is because taller buildings offer a larger facade area for BIPV integration, potentially increasing overall power generation. Climate zones with high solar radiation (1–3) seem to benefit most from facade BIPV in this scenario. In these zones, deeper facade profiles effectively balance energy savings through shading with substantial potential power generation due to ample sunlight exposure.

To further enhance the results, using high-resolution weather data customized for each location can better capture recent local climate conditions, thereby improving the accuracy and relevance of the study outcomes.

5. Limitations and future work

In this study, the PV-louver on south façade and PV-mounted rooftop systems were modeled using a combination of software tools, primarily utilizing the EnergyPlus code within the LB. The modeling approach

involved defining parameters such as irradiance levels, panel efficiency $(\eta_{PV}),$ and loss factors (LF). However, it's important to note that our simulation framework has limitations, particularly in accounting for temperature effects of operating such systems in real-world. Due to the constraints of the software used, we focused on key parameters that could provide meaningful insights into the performance of the PV system within the scope of our study. While acknowledging these limitations, we aimed to contribute novel findings regarding the overall energy behavior and potential PVPP of the PV louver system. Future research directions may explore advanced modeling techniques or alternative software tools capable of addressing these factors to enhance the accuracy and comprehensiveness of PV simulations.

CRediT authorship contribution statement

Hamideh Hossei: Writing – original draft, Visualization, Validation, Project administration, Methodology, Investigation, Formal analysis, Data curation, Conceptualization. **Kyoung Hee Kim:** Writing – review & editing, Validation, Supervision, Resources, Methodology, Funding acquisition, Conceptualization.

Declaration of competing interest

The authors declare the following financial interests/personal relationships which may be considered as potential competing interests: Kyoung-Hee Kim reports financial support and equipment, drugs, or supplies were provided by UNC Charlotte. If there are other authors, they declare that they have no known competing financial interests or personal relationships that could have appeared to influence the work reported in this paper.

Data availability

Data will be made available on request.

Acknowledgement

This study was funded by U.S. National Science Foundation (NSF). Award number: 2122014.

References

- [1] EIA. How much energy is consumed in U.S. buildings? 2023 [cited 2023; Available from: https://www.eia.gov/tools/faqs/faq.php?id=86&t=1.
- [2] J.D.S. Freitas, et al., Modeling and assessing BIPV envelopes using parametric Rhinoceros plugins Grasshopper and Ladybug, Renew. Energy 160 (2020) 1468–1479.
- [3] S. Aguacil, S. Lufkin, E. Rey, Active surfaces selection method for buildingintegrated photovoltaics (BIPV) in renovation projects based on self-consumption and self-sufficiency, Energ. Buildings 193 (2019) 15–28.
- [4] A. Azami, H. Sevinc, The energy performance of building integrated photovoltaics (BIPV) by determination of optimal building envelope, Build. Environ. 199 (2021) 107856.
- [5] T. Hwang, S. Kang, J.T. Kim, Optimization of the building integrated photovoltaic system in office buildings—focus on the orientation, inclined angle and installed area, Energ. Buildings 46 (2012) 92–104.
- [6] H. Yang, L. Lu. The optimum tilt angles and orientations of PV claddings for building-integrated photovoltaic (BIPV) applications. 2007.
- [7] C. Cheng, C.S.S. Jimenez, M.-C. Lee, Research of BIPV optimal tilted angle, use of latitude concept for south orientated plans, Renew. Energy 34 (6) (2009) 1644–1650.
- [8] B.D. Dimd, et al., Quantification of the impact of azimuth and tilt angle on the performance of a PV output power forecasting model for BIPVs, IEEE J. Photovoltaics (2023).
- [9] I.B. Rambøl, H.L.S. Vøllestad, M. Haugen. Building integrated photovoltaics in residential areas: a comparative study of energy performance at different orientations. 2023, NTNU.
- [10] K. Kim, et al. Performance assessment of a multifunctional 3D BIPV system. in ARCC 2023 International Conference. The Research-Design Interface. 2023.
- [11] A. Mesloub, G.A. Albaqawy, M.Z. Kandar, The OPTIMUM performance of Building Integrated Photovoltaic (BIPV) windows under a semi-arid climate in algerian office buildings, Sustainability 12 (4) (2020) 1654.

[12] N. Alhammadi, et al., Building-integrated photovoltaics in hot climates: experimental study of CIGS and c-Si modules in BIPV ventilated facades, Energ. Conver. Manage. 274 (2022) 116408.

- [13] H. Alrashidi, et al., Thermal performance evaluation and energy saving potential of semi-transparent CdTe in Façade BIPV, Sol. Energy 232 (2022) 84–91.
- [14] Z. Liu, et al., A comprehensive study of feasibility and applicability of building integrated photovoltaic (BIPV) systems in regions with high solar irradiance, J. Clean. Prod. 307 (2021) 127240.
- [15] Y. Sun, et al., Integrated semi-transparent cadmium telluride photovoltaic glazing into windows: energy and daylight performance for different architecture designs, Appl. Energy 231 (2018) 972–984.
- [16] Y. Cheng, et al., Investigation on the daylight and overall energy performance of semi-transparent photovoltaic facades in cold climatic regions of China, Appl. Energy 232 (2018) 517–526.
- [17] Y. Wang, Y. Chen, C. Li, Energy performance and applicability of naturally ventilated double skin façade with Venetian blinds in Yangtze River Area, Sustain. Cities Soc. 61 (2020) 102348.
- [18] S. Liang, et al., Design and performance validation on a solar louver with concentrating-photovoltaic-thermal modules, Renew. Energy 191 (2022) 71–83.
- [19] Y. Luo, et al., A comparative study on thermal performance evaluation of a new double skin façade system integrated with photovoltaic blinds, Appl. Energy 199 (2017) 281–293.
- [20] C. Zomer, et al., Performance assessment of partially shaded building-integrated photovoltaic (BIPV) systems in a positive-energy solar energy laboratory building: architecture perspectives, Sol. Energy 211 (2020) 879–896.
- [21] J. Huang, et al., Numerical investigation of a novel vacuum photovoltaic curtain wall and integrated optimization of photovoltaic envelope systems, Appl. Energy 229 (2018) 1048–1060.
- [22] S. Shi, et al., Energy-saving potential comparison of different photovoltaic integrated shading devices (PVSDs) for single-story and multi-story buildings, Energies 15 (23) (2022) 9196.
- [23] J. Kim, et al., Power performance assessment of PV blinds system considering self-shading effects, Sol. Energy 262 (2023) 111834.
- [24] A.L. Schmid, L.K.S. Uehara, Lighting performance of multifunctional PV windows, Energ. Buildings 154 (2017) 590–605.
- [25] A. Cannavale, et al., Improving energy and visual performance in offices using building integrated perovskite-based solar cells: a case study in Southern Italy, Appl. Energy 205 (2017) 834–846.
- [26] L. Olivieri, et al., Energy saving potential of semi-transparent photovoltaic elements for building integration, Energy 76 (2014) 572–583.
- [27] X. Su, et al., Energy performance of a reversible window integrated with photovoltaic blinds in Harbin, Build, Environ, 213 (2022).
- [28] C. Qiu, H. Yang, Daylighting and overall energy performance of a novel semitransparent photovoltaic vacuum glazing in different climate zones, Appl. Energy 276 (2020).
- [29] A. Riaz, et al., Experimental Study on Electrical Power Generation and Natural Daylighting Illuminance Due to Building-Applied Photovoltaic Façade Application. The International Symposium on Heating, Ventilation and Air Conditioning, Springer, 2019.
- [30] A. Shankar, K. Vijayakumar, B.C. Babu, Energy saving potential through artificial lighting system in PV integrated smart buildings, Journal of Building Engineering 43 (2021).
- [31] F. Roberts, et al., Effect of semi-transparent A-Si Pv glazing within double-skin façades on visual and energy performances under the UK climate condition. Available at SSRN 4098542, 2023.
- [32] H. Chen, et al., Study on natural lighting and electrical performance of louvered photovoltaic windows in hot summer and cold winter areas, Energ. Buildings (2022)
- [33] C. Xiang, B.S. Matusiak, Façade Integrated Photovoltaics design for high-rise buildings with balconies, balancing daylight, aesthetic and energy productivity performance, Journal of Building Engineering 57 (2022) 104950.
- [34] Y. Sun, et al., Analysis of daylight glare and optimal lighting design for comfortable office lighting, Optik 206 (2020) 164291.
- [35] ASHRAE, in lighting. 2019.
- [36] S.E., Daylight of buildings. 2019, European Committee for Standardization. 17037: 2019.
- [37] A. Nabil, J. Mardaljevic, Useful daylight illuminance: a new paradigm for assessing daylight in buildings, Light. Res. Technol. 37 (1) (2005) 41–57.
- [38] Power, R.G.E. Concentrated Solar Power (CSP) Vs Photovoltaic panels (PV). 2012 [cited 2024; Available from: https://www.renewablegreenenergypower.com/solar-energy/solar-energy-facts-concentrated-solar-power-csp-vs-photovoltaic-pv-panels.
- [39] Institute, B., BIPV Solutions in Europe: Competitiveness Status & Roadmap Towards 2030. 2021.
- [40] J.J. Cook, et al., Observations and Lessons Learned From Installing Residential Roofing-Integrated Photovoltaics. 2023, National Renewable Energy Lab.(NREL), Golden, CO (United States)
- [41] pvXchange. Preisindex. 2023 [cited 2023; Available from: https://www.pvxchange. com/Preisindex.
- [42] Jowett, P. European Parliament approves legal requirement to install solar on buildings. 2024 [cited 2024; Available from: https://www.pv-magazine.com/2024/03/13/european-parliament-approves-legal-requirement-to-install-solar-on-buildings/.
- [43] Energy, E.S. Europe's industrial revolution for efficient buildings: shaping the future. 2024 [cited 2024; Available from: https://www.pv-magazine.com/press-releases/europes-industrial-revolution-for-efficient-buildings-shaping-the-future/.

- [44] Senate Department for Economic Affairs, E.a.P.E. Berlin solar law. 2024 [cited 2024; Available from: https://www.berlin.de/sen/web/en/.
- [45] Office, S.E.T. Solar Energy Guide for Homebuilders. 2023 [cited 2024; Available from: https://www.energy.gov/eere/solar/solar-energy-guide-homebuilders.
- [46] H.C. Curtius, The adoption of building-integrated photovoltaics: barriers and facilitators, Renew. Energy 126 (2018) 783–790.
- [47] W. Feng, et al., A review of net zero energy buildings in hot and humid climates: experience learned from 34 case study buildings, Renew. Sustain. Energy Rev. 114 (2019) 109303
- [48] H. Hossei, K.-H. Kim, Circuit Connection Reconfiguration of Partially Shaded BIPV Systems, a Solution for Power Loss Reduction. In ACSA Annual Meeting in Common, 2023.
- [49] Y. Gao, et al., A photovoltaic window with sun-tracking shading elements towards maximum power generation and non-glare daylighting, Appl. Energy 228 (2018) 1454–1472
- [50] E. Taveres-Cachat, et al., A methodology to improve the performance of PV integrated shading devices using multi-objective optimization, Appl. Energy 247 (2010) 731 744
- [51] M.A. Paydar, Optimum design of building integrated PV module as a movable shading device, Sustain. Cities Soc. 62 (2020) 102368.
- [52] R. Ito, S. Lee, Development of adjustable solar photovoltaic system for integration with solar shading louvers on building façades, Appl. Energy 359 (2024) 122711.
- [53] Y. Cheng, et al., An optimal and comparison study on daylight and overall energy performance of double-glazed photovoltaics windows in cold region of China, Energy 170 (2019) 356–366.
- [54] A.M.E.A. Akata, D. Njomo, B. Agrawal, Assessment of building integrated photovoltaic (BIPV) for sustainable energy performance in tropical regions of Cameroon, Renew. Sustain. Energy Rev. 80 (2017) 1138–1152.
- [55] H. Li, S. Wang, H. Cheung, Sensitivity analysis of design parameters and optimal design for zero/low energy buildings in subtropical regions, Appl. Energy 228 (2018) 1280–1291.

- [56] ASHRAE. ASHRAE Climate Zones. 2011 [cited 2024; Available from: https://openei.org/wiki/ASHRAE Climate Zones.
- [57] F. Goia, Search for the optimal window-to-wall ratio in office buildings in different European climates and the implications on total energy saving potential, Sol. Energy 132 (2016) 467–492.
- [58] (NREL), N.R.E.L. PVWatts V8. 2020 [cited 2024; Available from: https://developer.nrel.gov/docs/solar/pvwatts/v8/.
- [59] Associates, R.M. Rhino 8. 2024 [cited 2024; Available from: https://www.rhino3d. com/.
- [60] N. Skandalos, D. Karamanis, An optimization approach to photovoltaic building integration towards low energy buildings in different climate zones, Appl. Energy 295 (2021) 117017.
- [61] Chris Machey. LADYBUG TOOLS 2022; Available from: https://www.food4rhino.com/en/app/ladybug-tools.
- [62] Energy, U.S.D.o., EnergyPlus™ Version 22.1.0 Documentation. Engineering Reference. 2022.
- [63] DOE. Weather Data. 2024; Available from: https://energyplus.net/weather.
- [64] Solemma. ClimateStudio. 2022 [cited 2022; Available from: https://www.solemma.com/climatestudio.
- [65] M.Z. Jacobson, V. Jadhav, World estimates of PV optimal tilt angles and ratios of sunlight incident upon tilted and tracked PV panels relative to horizontal panels, Sol. Energy 169 (2018) 55–66.
- [66] A.H. Alami, et al., Management of potential challenges of PV technology proliferation, Sustainable Energy Technol. Assess. 51 (2022) 101942.
- [67] A.P. Dobos. PVWatts version 5 manual. 2014, National Renewable Energy Lab. (NREL), Golden, CO (United States).
- [68] D.D. Milosavljević, T.S. Kevkić, S.J. Jovanović, Review and validation of photovoltaic solar simulation tools/software based on case study, Open Physics 20 (1) (2022) 431–451.
- [69] I.L. Handbook, IES Lighting Handbook, Illuminating Engineering Society, New York, 1966.